Late Pleistocene paleoenvironment at a Middle Stone Age archaeological site in Equatorial Guinea: a paleopedological approach

Paleoambiente pleistocénico tardío en un sitio arqueológico del Mesolítico de Guinea Ecuatorial: un enfoque paleopedológico

Tamara **Cruz-y-Cruz**[1,2,*], Alejandro **Terrazas-Mata**[3], Lilit **Pogosyan**[4], Sergey **Sedov**[5], Teresa **Pi-Puig**[5,6], Iran **Rivera-González**[2], Beatriz **Menéndez-Iglesias**[1,7], Jorge **Rodríguez-Rivas**[8], Héctor **Cabadas-Báez**[9]

[1] Postdoctoral Scholarship Program, National Autonomous University of Mexico (UNAM), Scholar of the Institute of Anthropological Research. Ciudad Universitaria, 04510, CDMX, Mexico.

[2] National School of Anthropology and History (ENAH-INAH), Periférico Sur y Zapote sn. Isidro Fabela, Tlalpan, CDMX, Mexico.

[3] Institute of Anthropological Research, UNAM, Ciudad Universitaria, 04510, CDMX, Mexico.

[4] Faculty of Soil Science, Moscow State University, Leninskie Gory 1-12, 119991, Moscow, Russia.

[5] Institute of Geology, UNAM, Ciudad Universitaria, 04510, CDMX, Mexico.

[6] National Laboratory of Geochemistry and Mineralogy (LANGEM), Institute of Geology, UNAM, Ciudad Universitaria, 04510, CDMX, Mexico.

[7] Gerda Henkel Foundation. Patrimonies Funding Initiative, Düsseldorf, Germany.

[8] UNAM Project "Early Homo sapiens Settlement in the Tropical Rainforests of Equatorial Guinea".

[9] Geology Laboratory, Faculty of Geography, Autonomous University of the State of Mexico, Cerro Coatepec s/n Ciudad Universitaria, 50110, Toluca, Estado de México, Mexico.

* Corresponding author: (T. Cruz-y-Cruz) *tamczyc@yahoo.com.mx, tamara_cruz@inah.gob.mx*

How to cite this article:
Cruz-y-Cruz, T., Terrazas-Mata, A., Pogosyan, L., Sedov, S., Pi-Puig, T., Rivera-González, I., Menéndez-Iglesias, B., Rodríguez-Rivas, J., Cabadas-Báez, H., 2022, Late Pleistocene paleoenvironment at a Middle Stone Age archaeological site in Equatorial Guinea: a paleopedological approach: Boletín de la Sociedad Geológica Mexicana, 74 (3), A200622. http://dx.doi.org/10.18268/BSGM2022v74n3a200622

Manuscript received: December 12, 2021.
Corrected manuscript received: June 20, 2022.
Manuscript accepted: June 23, 2022.

Peer Reviewing under the responsibility of Universidad Nacional Autónoma de México.

ABSTRACT

Key evidence of human occupation in Africa during the Middle Palaeolithic (*Middle Stone Age* [MSA]) is available from the south and east of the continent, where semi-arid climate prevails. Rare evidence of MSA human occupation in the humid tropical region was recently reported from Equatorial Guinea. To identify if paleolithic human occupation occurred in the tropical forest, the stratigraphy of the recently discovered archaeological site "Mabewele I" was analyzed using a paleopedological approach. The properties evaluated along a vertical profile are: granulometry, magnetic susceptibility (*K*), free iron extractable with sodium dithionite (Fe_d), total organic carbon (TOC), chemical composition by X-ray fluorescence (XRF), X-ray diffraction mineralogy (XRD), ternary plot of the three main oxides (SiO_2-Al_2O_3-Fe_2O_3), phytoliths and micromorphology. The predominant fraction is sand, with a significant clay content (> 30 %). The *K* and the Fe_d presented low values, as well as the TOC. XRF showed few variations along the sequence and XRD showed that the clays are mainly kaolinites, with a very low component of vermiculites. The phytoliths correspond to tropical vegetation with few changes in the vegetal composition between the deep and superficial zones. A charcoal from the lower part of the profile was dated between 12.57-12.24 ka cal BP, while the main artifact horizon was located at the bottom. The analytical results appear contradictory: on the one hand, there is evidence of intense chemical weathering under a humid tropical climate, but the clay cutans in the pores are very scarce and incipient and the iron nodules are mostly anorthic. This indicates that the sequence is composed of pedosediments associated with a high environmental dynamism, with short periods of erosion-sedimentation-pedogenesis. The results allow us to propose that humans inhabited the tropical forest during the MSA and that erosion-sedimentation processes could be related to anthropization processes.

Keywords: Middle Stone Age, Equatorial Guinea, rainforest, paleopedology.

RESUMEN

Las principales evidencias de ocupación humana en África durante la Edad de la Piedra Media (Middle Stone Age –MSA-) *se han hallado en el sur y el este del continente, en las regiones de climas secos. Sin embargo, investigaciones recientes en la región tropical de Guinea Ecuatorial han hallado artefactos arqueológicos de dicho periodo. Para identificar si la ocupación humana paleolítica ocurrió en la selva tropical, se analizó la estratigrafía del sitio arqueológico "Mabewele I", recientemente descubierto, bajo un enfoque paleopedológico. Las propiedades evaluadas fueron: granulometría, susceptibilidad magnética, hierro libre extractable con ditionito de sodio (Fe_d), carbono orgánico total (TOC), composición química por Fluorescencia de rayos X (FRX), mineralogía por difracción de rayos X (DRX), fitolitos y micromorfología. La fracción predominante es la arena, con un contenido de arcillas importante. La K y el Fe_d presentaron valores bajos, al igual que el TOC. La FRX mostró pocas variaciones a lo largo de la secuencia y la DRX indicó que las arcillas son principalmente caolinitas, con un componente muy bajo de vermiculitas. Los fitolitos corresponden a vegetación tropical, con pocos cambios en la composición vegetal entre las zonas profunda y superficial. Un carbón de la parte baja del perfil fue datado entre 12.57-12.24 ka Cal AP, mientras que los artefactos fueron localizados al fondo. Los resultados analíticos son contradictorios: por un lado, hay evidencias de intemperismo químico intenso bajo un clima tropical húmedo, pero los cutanes de arcilla en los poros son muy escasos e incipientes y los nódulos de hierro son mayormente anórticos. Ello indica que la secuencia se compone de pedosedimentos asociados a un alto dinamismo ambiental, con cortos periodos de erosión-sedimentación-pedogénesis. Los resultados permiten proponer que los humanos habitaron la selva tropical durante el MSA y que los procesos de erosión-sedimentación podrían estar relacionados con procesos de antropización.*

Palabras clave: Edad de Piedra Media, Guinea Ecuatorial, selva tropical, paleopedología.

http://dx.doi.org/10.18268/BSGM2022v74n3a200622

1. Introduction

Although *Homo sapiens* originated in Africa, it has long been considered that modern humans colonized the African rainforest only at the end of Pleistocene and mainly in the Holocene, when agriculture was introduced (Hart and Hart, 1986; Headland, 1987; Bailey and Peacock, 1988). However, recent archaeological studies at Central African sites demonstrate human presence during the late Pleistocene in regions that are today covered by rainforest (Martí, 1999; Cornelissen *et al.*, 2002). Unfortunately, only some sites are properly recorded, preserved, and dated. In addition, some sites that are now covered by forest could have been occupied with open woodland or savanna vegetation during periods with drier and cooler environments (Taylor, 2016). To close this gap, it is necessary to investigate prehistoric sites located in tropical regions that contain pre-ceramic and pre-Iron Age artifacts, to establish the environmental conditions at the time of human occupation.

In general, the tropical regions of Africa (including the part occupied at present by the humid forest ecosystems) are known to experience large-scale environmental changes linked to the global climatic cycles of the late Pleistocene. During several decades of research, the paleoecological models have been modified significantly. Until the 1960s prevailed the idea of moister conditions in African tropics (pluvial periods) during the glacial periods – explained by the drop of temperature, decrease of evaporation and shift of more humid environments towards the equator; however, at that time evidence of the opposite trend started to increase (see *e.g.*, Van Zinderen Bakker, 1966). In the next decade the idea of aridization as a main paleoclimatic trend in the African tropics during the last glaciation became dominant, being supported by various records, in particular – distribution of sand dunes (Sarnthein, 1978). It provoked severe changes in landscape and huge area of rainforests has been replaced by savanna, leaving the rainforest in few small and separated oases (Adkins *et al.*, 2006). In recent studies the territory of Equatorial Guinea is considered being one of such oases (see *e.g.*, Steele, 2013). Dry conditions of the Last Glacial Maximum were sharply reversed and followed by the African Humid Period during the Late Glacial – middle Holocene (COHMAP Members, 1988; Adkins *et al.*, 2006). During this period, fluctuations in the expansion of tropical rainforests occurred several times (Maley, 1991) and then the humid period ended sharply at about 5.5 ka BP (deMenocal *et al.*, 2000). Towards the late Holocene, the trend towards the shrink of the forests and increase of savanna-type vegetation is documented, caused by climatic changes (Ngomanda *et al.*, 2009). The Meghalayan stage of the Holocene is characterized by increase of human settlements along the northwestern margin of the Central African Rainforest, but the rainforest suffered considerable changes due to environmental degradation, so the pollen records showed that in some episodes there was higher proportion of light-demanding trees (Lezine *et al.*, 2013). Taking into consideration this rather complex Late Quaternary climatic history on the continental scale we consider very important the search of archaeological and paleoecological records in the territories, where the climatic fluctuations were not so contrasting and refugia of forest could persist throughout late Pleistocene. Recently, in the continental territory of Equatorial Guinea, lithic artifacts from MSA diagnoses have been recovered, with a minimum age of 30 ka (Mercader and Martí, 2002; Mercader, 2002; Terrazas and Rosas, 2016). Because the Montes Camerún–Monte Alen–Monte Mitra–Montes de Cristal region (Figure 1) has one of the highest rates of biodiversity and botanical endemism in Africa, it is considered that environmental conditions have not changed since the Miocene (Hamilton, 1976; Hamilton and Taylor, 1991; Plana, 2004); however, this has not been corroborated with paleoclimatic records. For this reason, in this article we present the first paleopedological studies and paleoenvironmental interpretations of a preceramic archaeological site in Equatorial Guinea.

For this, the section of the "Mabewele I" site that contained lithic artifacts from the Sangoan / Lupemban traditions of the MSA of Central

http://dx.doi.org/10.18268/BSGM2022v74n3a200622

Africa was analyzed under a multiproxy paleopedological approach, to identify origin of the materials that form the sequence (soil and/or sediments) as well as the time span of their formation, considering the characteristic times of the pedological processes identified (Targulian and Krasilnikov, 2007).

2. Study area

Equatorial Guinea is located on the west coast of Africa, on the equator (Figure 1). The country is made up of continental territory and two islands. The mainland is bordered to the north by Cameroon, to the east and south by Gabon and to west by the Gulf of Guinea, where the islands of Bioko and Annobón are located (IUCN, 1991). The investigation was carried out in the mainland, in the Niefang District.

The relief of the study area is dominated by the Monte Alen-Monte Mitra mountain range, the Wele River, which runs from east to west, and the Uoro Rift, which runs from northeast to southwest (Figure 1). The main rocks are granulite gneiss, quartziferous diorites, and granites (Martínez-Torres and Riaza, 1996; Alvar *et al.*, 1996). The soil types in the region are mainly Ferralsols, Acrisols, and Nitisols (De Castro and De la Calle, 1985; IUCN, 1991; Da Costa *et al.*, 2015).

Current climate is equatorial. The mainland has two dry seasons, one between December and

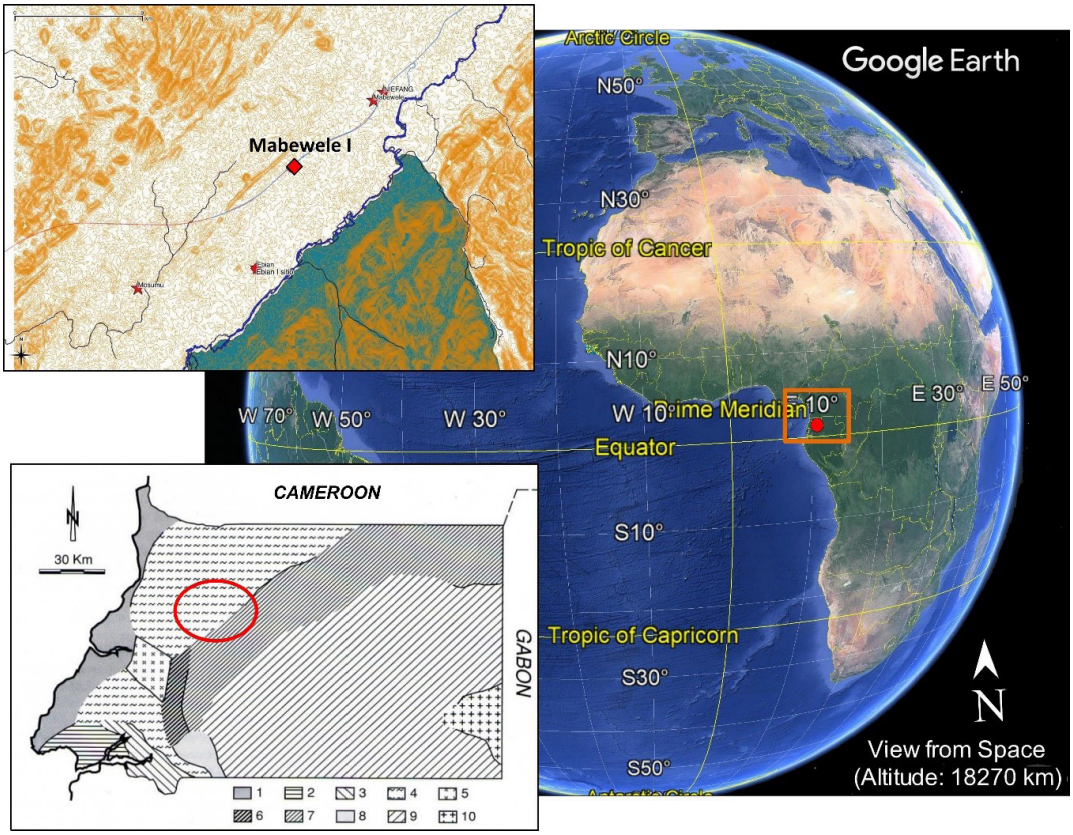

Figure 1 Location of the Equatorial Guinea in Africa. The red dot on the satellite image shows the location of Equatorial Guinea in Africa and the orange line indicates the Montes Camerun - Monte Alen - Monte Mitra – Montes de Cristal region (modified from Google Earth Pro 2022). On the left is the map of the general geology of continental Equatorial Guinea: 1) Tertiary; 2) sandstones and shales (Cretaceous): 3) sublitoral sandstones (Cretaceous; 4) gneiss; 5) fine-grained gneiss (leptites); 6) hyperstene with quartz diorites; 7) quartz diorites: 8) gabbro; 9) coarse-grained granite; 10) fine-grained granite. The red circle shows the study area (Modified from: Martínez-Torres and Riaza, 1996). In the upper box, the location of Mabewele I is shown with a red dot.

http://dx.doi.org/10.18268/BSGM2022v74n3a200622

February and another between July and September as well as two rainy seasons between March and June and between September and November, respectively. Average annual temperature is 25° C, with relative humidity of 90% and average annual rainfall is 1500-7000 mm. The wettest areas are found in Monte Mitra and the Mitemele basin (De Castro and De la Calle, 1985; Alvar *et al.*, 1996).

Vegetation is made up of primary forest (tropical rainforest), with specimens such as okumé (*Aucoumea klaineana*), ceiba (*Ceiba pentandra*) and secondary vegetation due to anthropogenic activity (Velayos *et al.*, 2014; Díaz *et al.*, 2016; IUCN, 1991). The areas where the primary forest is still conserved are the Niefang Chain (inside Monte Alen National Park) and the southeastern of the country (IUCN, 1991). In this area, biological diversity is high, made up of large mammals such as forest buffalo, chimpanzees, and elephants, as well as other smaller species.

3. Materials and Methods

"Mabewele I" archaeological site, was located in 2016 and excavated in 2017 and 2019. There geographic coordinates are N 1°18'10.7" and E 10° 10´30.10", at 325 m above sea level (a.s.l.). The site is 4 km southwest of Niefang, close to the Bata-Niefang highway, which extends over a plain formed on an alluvial terrace. The area belongs to Mabewele County and is in the Uoro Depression Physiographic Region (IUCN, 1991).

3.1. FIELD RESEARCH

The fieldwork included several surveys in the area to identify archaeological materials exposed on the surface and/or visible in the cuts of the land, as well as to identify the presence of associated soils and/or paleosols.

The surface survey revealed that during the construction of the Bata-Niefang highway, a 20-meter embankment was cleared on each side of the road, revealing numerous stone artifacts (Figure 2).

It was also observed that during these works the vegetation and the superficial horizon were removed to level the terrain. The cuts in the ground made it possible to observe that the base of the materials remained intact, so we carried out an archaeological excavation to recover them (Fig-

Figure 2 **Image of the open-air site of mabewele I: the brown line marks the area of distribution in the surface of the lithic artifacts, the blue line marks a small seasonal stream; the blue square marks the excavation area at the highest point of the site (modified from Google Earth Pro 2022).**

http://dx.doi.org/10.18268/BSGM2022v74n3a200622

ure 3). The excavation covered four square meters in surface and was carried out in two seasons, the first in 2017 and the second in 2019.

3.1.1. ARCHAEOLOGICAL RESEARCH

For the archaeological excavation, stratigraphic control was executed by metric levels of 10 cm. The archaeological materials found consisted of lithic artifacts arranged along the profile, although the highest concentration of artifacts was in the lower part of the excavation pit. Artifacts recovered from each level were georeferenced and located in three dimensions (x, y and z) in a local reference system for the site. Deep were recorded manually, fixing each point with Bosch PLL 1P model line laser level, fixed in the central milestone of the site, in the highest point of the terrain, one meter over the ground and measuring the deep to from a reference level. Preferential orientation and inclination of each lithic artifact were recorded to identify possible displacement of the materials and sediments in the relief.

3.1.2. PALEOPEDOLOGICAL RESEARCH

While the archaeological excavation was carried out, the west and south profiles of the excavated pit were described with a pedological approach, for paleopedological and paleoenvironmental studies.

In 2017, western profile was described from the surface to a depth of 1.6 m, to the stone line where the artifacts were found; and in 2019 was

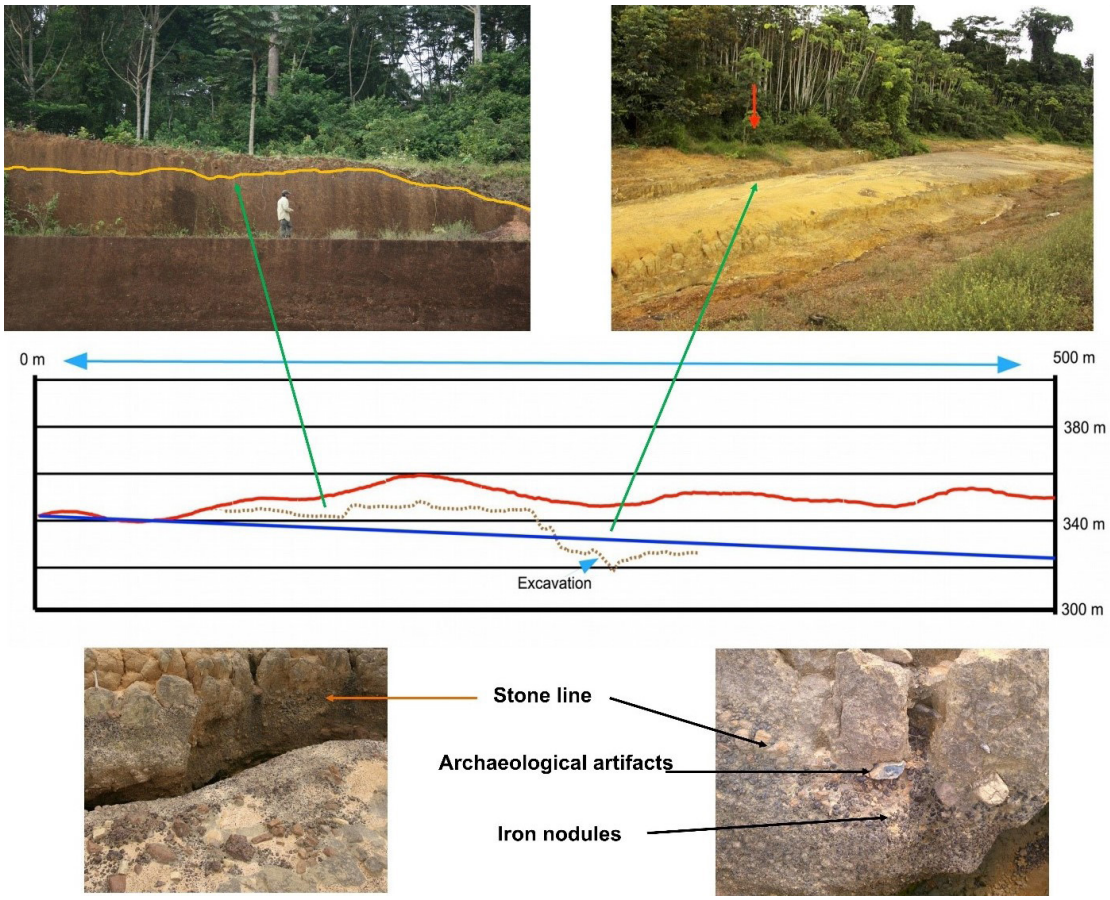

Figure 3 Section of the Bata-Niefang highway, showing the modern surface (red line), the location of the stoneline and archaeological artifacts (brown dotted line), the surface of the highway (blue line) and the position of the excavation. In the images above: the position of the Stone line on the ground is shown on the left with a yellow line and the excavation site is indicated on the right with a red arrow. The lower images show details of the Stone line, with iron nodules and some archaeological artifacts.

http://dx.doi.org/10.18268/BSGM2022v74n3a200622

described southern profile up to 1.73 m, including the stone line and reaching saprolite. The stone line is continued in both directions allowing note that the lithic artifacts were deposited thereon (Figure 3).

Both profiles were described based on the FAO (2006) guidelines for soil horizons description: depth, horizon boundaries, color, texture, structure, consistency, porosity, organic matter, cutans, stains and concretions and presence of carbonates using HCl at 10%.

In total, eleven horizons were identified and described: Bo/2C/3C/4Bo/5Bo/6Bo/7Bo/8Bo /9Buo/10Bco/11CB, from which samples were collected to analyze their physical and chemical properties, as well as undisturbed samples for micromorphological analysis.

3.2. LABORATORY RESEARCH

The samples were processed in the laboratories of the Institute of Geology of the National Autonomous University of Mexico, where the physical and chemical characteristics were evaluated (Targulian and Krasilnikov, 2007).

3.2.1. PROPERTIES EVALUATED

The particle size analysis was applied to the entire sequence, except for 2C and 3C horizons. The analyzes of magnetic susceptibility (*K*), free iron extractable with sodium dithionite (Fe_d) and Total Organic Carbon (TOC), were applied only to Bo, 4Bo-9Buo horizons; while the identification of clays by XRD, elemental quantification by XRF, ternary plot of the three main oxides (SiO_2-Al_2O_3-Fe_2O_3) and micromorphological analysis were applied to the entire sequence.

1. Particle size analysis was accomplished with the pipette method, giving the samples previous treatments to remove cementitious materials (H_2O_2 at 30% to remove organic matter, HCl to remove any carbonates they might contain, treatment with citrate-bicarbonate-dithionite to remove iron oxides, and sodium hexametaphosphate to disperse particles), based on Buol *et al.* (1981) and Mehra and Jackson (1960).

2. Low and high frequency magnetic susceptibility (K_{lf} and K_{hf}) was measured with a Bartington MS2 susceptiblity meter, according to Dearing *et al.* (1996).

3. Free iron was evaluated by selective extraction with citrate-bicarbonate-dithionite (Fe_d), based on Mehra and Jackson (1960). The samples were analyzed in duplicate, and the average was considered for the interpretation of the results.

4. Total organic carbon (TOC) was quantified in duplicate on a CHNS / O Perkin Elmer 2400 series II elemental analyzer, in CHN mode, using helium as a carrier gas at a combustion temperature of 980° C and a reduction temperature of 640° C, with a thermal conductivity detector.

5. Clays from all horizons was identified and total mineralogical composition of two samples was studied by XRD. For whole rock analysis, samples were ground in an agate mortar, sieved to less than 45 microns and loaded on aluminum sample holders. For the identification of clays, the cementing agents were removed to disperse the particles and the clay fraction was extracted according to Stoke's law (Jackson, 1958; Moore and Reynolds, 1997). The prepared samples were mounted on glass slides, dried at 30 °C (Moore and Reynolds, 1997) and solvated with ethylene glycol at 70 °C for 24 hours. Bulk rock phase identification and quantification by Rietveld method (Rietveld 1969) was made using Highscore v4.5 software (Malvern, UK), using International Center of Diffraction Database (ICDD) and Inorganic Crystal Structure database (ICSD). Kaolinite has been identified by (001) peak at 12.5° 2θ (~7Å) in the air-dried and glycolated samples. By heating to 550°C kaolinite becomes amorphous and its diffraction pattern disappears. The presence of few vermiculites in the samples was confirmed by (001) reflection at about 6°2θ (~14Å) in the air-dried condition that was not affected by ethylene glycol treatment and collapsed to 10 after heating at 550°C.

6. Major elements and trace elements were identified by XRF. The major elements were measured in molten sample with 90% by weight of $Li_2B_4O_7$. Loss on calcination (PXC) was determined by heating 1g of sample at 950° C for 2 hours and calculating the difference in mass in percent. Trace element analysis

http://dx.doi.org/10.18268/BSGM2022v74n3a200622

Table 1. Analysis of the archaeological artifacts of Mabewele.

	Small Nodules <5cm diameter	Middle sized Boulders 5-10cm diameter	Big Nodules >10cm diameter	Dark Quartzite Slabs	Grey Quartzite Slab	Total
Slab Cores				11		11
Polyhedral cores	4	11				15
Levallois Cores		6	8			14
Scrappers				2		2
Tranchet				2		2
Retouched Polyhedral Cores	1			11		12
Bifacial Knife with reserved base				3	1	4
Bifacial Knife				11	1	12
Trihedral Pick				2		2
Chopper on Slab				3		3
Core-axe				4		4
Primary Blanks	37	1	9	13		60
Secondary Blanks	29	7	41	35		112
No cortex Blanks	10	2	45	11		68
Discoidal on Flake					1	1
Quadrangular Bifacial on Flake				2		2
Retouched Notch		1				1
Total	81	28	103	110	3	325

was performed on a pressed sample with 15% wax-C.

7. Ternary plot of the three main oxides (SiO_2-Al_2O_3-Fe_2O_3) was calculated to know the general weathering trend, according to Hill *et al.* (2000). Additionally, to evaluate the affinity with the parent material and detect lithological discontinuities within the studied sequence, the ternary plot Zr-Cr-Ti was considered, modified from Mounteney *et al.* (2018).

8. Radiocarbon dating was made using accelerator mass spectrometry (AMS), in charcoal remains recovered during the excavation. The sample was analyzed at the National Laboratory of Mass Spectrometry with Accelerators (LEMA, for its acronym in Spanish) of the National Autonomous University of Mexico (UNAM). The obtained date was calibrated with the radiocarbon calibration program Calib7.1.0, at 2σ.

9. Micromorphological analysis. For this analysis, thin sections from all horizons were observed with an Olympus America petrographic microscope, using transmitted plain polarized light (PPL), crossed polarized light (XPL) and reflected light. The pedological features observed in the materials were: matrix, fresh and/or degraded plant residues, humified organic matter, coatings, stains, nodules and/or concretions, weathering features (mineral etching, and alteration), among others (Stoops *et al.*, 2018).

http://dx.doi.org/10.18268/BSGM2022v74n3a200622

10. Phytolith extraction was processed based on Madella *et al.* (2005). Organic matter was removed using H_2O_2 (30%) and carbonates with HCl (0.5%), sodium dithionite were added to reduce free iron (Deb,1950); sodium hexametaphosphate was used for particle dispersion. A polytungstate solution was applied to recover phytoliths (2.6 g/cm^3 density) and observed under 100 X using a Dialux 20 microscope.

4. Results

4.1. FIELDWORK RESULTS

4.1.1. "MABEWELE I" ARCHEOLOGY

Among the materials recovered during the surface survey, were found *levallois* cores, polyhedral cores, and tabular cores, *levallois* flakes, centripetal extraction flakes and irregular flakes, as well as different "core tools", MSA points, bifacial knives, tranchets and discoid, made from quartzite and quartz. The raw materials of the artifacts were extracted from quartzite slabs, as well as small boulders. All surface tools correspond to the MSA (according with definition for Equatorial Guinea from Mercader and Martí 1999, 2002). No pottery, blades or microliths were recorded at the site. Results are summarized on table 1.

Although some scattered quartzite chips were recorded in all horizons, most flakes and chips were concentrated in the horizon 9Buo and in the area of contact with 10Bco. This horizon (10Bco) is a conglomerate of iron oxide nodules that make up the "stone line" (Mercader *et al.*, 2002) and flakes and chips inside come from 9Buo due to vertical displacement. Therefore, 9Buo is the only archaeological level of the excavation. In this layer, a *levallois* flake fractured in half, several irregular centripetal extraction flakes, unifacial and bifacially retouched flakes and numerous non-diagnostic flakes and chips, made on polyhedral and *levallois* cores and flat tablet cores (Figure 4) were recorded. The raw material is like some surface materials (preliminary identified as quartzite).During the excavation, some lithic artifacts were found in small concentrations, with "fresh" edges that show no erosion or wear by natural processes.

There are even some sets of flakes that can be rejoined (Figure 5). In addition, the inclination and orientation of each flake were registered, to evaluate the degree of alteration and movement of the

Figure 4 Middle Stone Age diagnostic artifacts (MSA *ca.* 250-30 ka BP), collected on the surface: a) trihedral peak; b) tranchet; c and d) MSA points; e) bifacial core-tool; f and g) cores Levallois; h) discoidal core; i) Levallois flake, made in quartzite.

http://dx.doi.org/10.18268/BSGM2022v74n3a200622

lithic artifacts inside the sediment (Figure 6). In this way, the analysis of the spatial distribution showed that most of them present a preferential orientation of their major axes, which indicates that they were deposited by a flow of materials. However, most of the pieces are in a horizontal position, which suggests, along with the erosion-free condition of the edges, that the displacement was very short, and the artifacts are not far from where they were originally abandoned.

4.1.2. PALEOPEDOLOGICAL DESCRIPTION

Southern and western profiles of the archaeological excavation were described (Figure 7). In 2017 the western profile was described to the depth of 160 cm and in 2019 the description was completed to the depth of down to a saprolite level (173 cm). The description of the south profile confirmed the identification of horizons made in the west profile. The detailed morphological description of the excavated profile is presented in table 2.

Although at first glance the described sequence seems to be highly weathered homogenous material, pedological characteristics like structure, roots presence, moisture retention, high clay content and iron oxides among others are presented in this profile and allow dividing it into 11 different horizons. Single archaeological artefacts were found at surface level and among the entire pit and their occurrence highly increased at the lower part. In 2016, the study area was affected by road construction, so the upper part of the modern soil was stripped away by excavators and the Bo horizon was exposed to the surface, it was soon partially covered by vegetation (Figure 3). There are many archaeological artefacts that rest all over the surface of the eroded area.

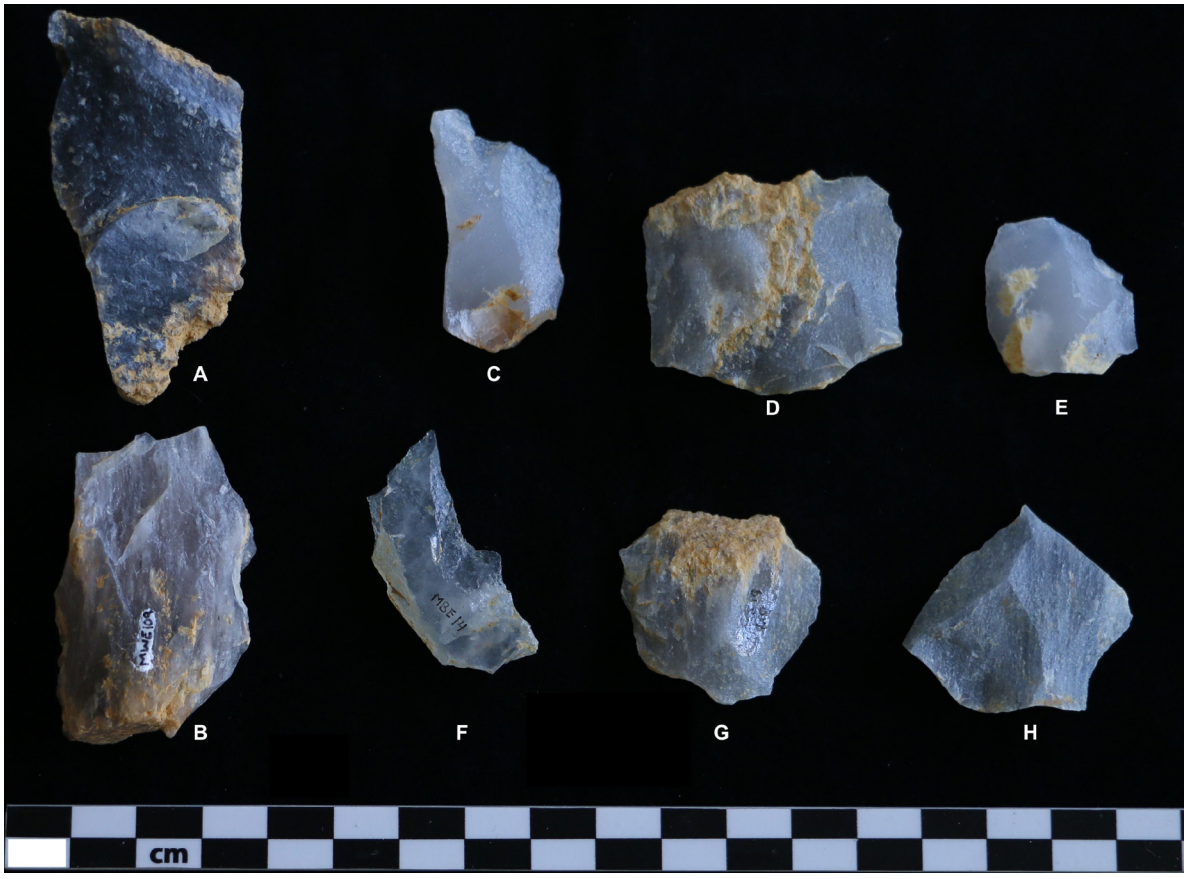

Figure 5 A and B, Quartzite cores; C, Levallois flake (broken) white quartz; D, Quartzite Flake; E, Levallois quartzite flake; F, Quartz flake; G, Quartzite flake; H, Levallois quartzite flake.

http://dx.doi.org/10.18268/BSGM2022v74n3a200622

The topsoil Bo horizon presents clay and iron oxides accumulation. Below it there are two light coloured layers of redeposited sorted quartz sand: 2C which is also different in color and 3C with a light inclination (15°) from NW to SE and they cover the sequence of several Bo horizons with more similar characteristics (they are clayey materials, compact, with good structure, enriched in iron, but they also contain a high proportion of coarse fraction, anortic iron nodules and lithic fragments with preferential orientation, for which they were identified as eroded soils and classified as Bo horizons). The 4Bo horizon is more indurated in comparison to the underlying 5Bo and 6Bo and the 5Bo has a higher content of sand. The horizons 7Bo, 8Bo and 9Buo are richer in clay and moisture content by contrast to upper-lying 5Bo and 6Bo horizons, but their density is lower. Common separated iron nodules start to appear in the 9Buo horizon and form the so called "stone line" in 10Bco. At the same time, the concentration of lithic artefact starts to increase in the 9Buo horizon and reaches its maximum at the 10Bco horizon where they rest on the top of the stone line. At the bottom of the excavation there is a white, strongly weathered saprolite from gneiss (11CB horizon).

4.2. ANALYTICAL RESULTS

The analytical results are shown in figure 8.

4.2.1. PARTICLE SIZE

Particle size analysis showed that the predominant fraction in almost all the samples is sand (> 50%), except in 9Buo (47.7%); however, the clay content is very high in all horizons (> 30%), while silt is the minority fraction, with less than 17%.

4.2.2. MAGNETIC SUSCEPTIBILITY

Magnetic susceptibility (K) was measured only in the western profile and presents extremely low values, with no substantial changes throughout the sequence. Values range from 3.7 to 6.7 units (K_{lf} x 10^{-5} IS) and from 2.9 to 5.3 units (K_{hf} x 10^{-5} IS). This indicates that the analyzed materials contain low or non-magnetic minerals.

4.2.3. FREE IRON CONTENT (Fe_d)

Free iron content (Fe_d) is very similar throughout the sequence (between 13.89 mg/g in 4Bo and 15.99 mg/g in 9Buo). A gradual increase is observed from the 4Bo horizon to deeper horizons; however, no correspondence is observed with the results of magnetic susceptibility, indicating that the iron oxides sides in the samples have very low magnetic susceptibility.

4.2.4. TOTAL ORGANIC CARBON (TOC)

As expected for Bo horizons of tropical soils, Total Organic Carbon (TOC) content was very low in all samples, with the maximum value in Bo

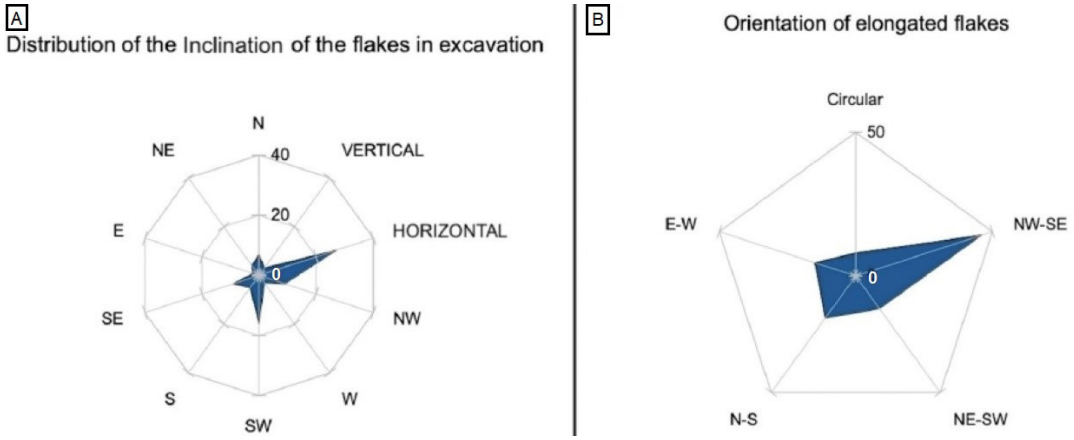

Figure 6 A: Inclination of artifacts in sediment; most were found in a horizontal position. B: Orientation of lithic artifacts in the sediment; most were found oriented in a NW-SE direction.

http://dx.doi.org/10.18268/BSGM2022v74n3a200622

(0.63%) and the minimum in 8Bo (0.29%), with a clear decrease towards the base of the profile.

4.2.5. X-RAY DIFFRACTION (XRD)

A semiquantitative analysis was performed by XRD to the total sample of Bo and 4Bo horizons (Table 3), considering that they correspond to different times of deposition and pedogenesis, separated by 2C and 3C. The results showed that both samples are mainly composed of three mineralogical components: quartz (Bo 87% and 4Bo 90%); kaolinite (Bo 9% and 4Bo 7%), and gibbsite (Bo 4% and 4Bo 3%). XRD analysis of the clay fraction allowed to identify, in addition to kaolinite, the presence of vermiculite, which in the quantification of the total sample was not perceived because it was found in very little quantity (Table 4; Figure 9).

4.2.6. X-RAY FLUORESCENCE (XRF)

Quantification of total elements by XRF (Figure 10a) showed that the materials contain predominantly silica -SiO_2- (> 75%), with the minimum values in the Bo horizons and the maximum values in the C horizons. Alumina (Al_2O_3) and total iron (Fe_2O_{3t}) show a contrary trend, with the maximum content in 9Buo and the minimum in 11CB. Titanium (TiO_2) does not vary much throughout the profile, with maximum values at 8Bo and minimum at 11CB. The other elements are found in smaller quantities and show little difference in general trends.

Trace elements (Figure 10b) showed clear differences between saprolite and soil material. The most evident change was observed in the content of Rb, Ba and Y, with maximum values in 11CB (saprolite) and a drastic decrease in the other horizons, while the content of Sr, Th, Pb, or Zr, showed the opposite trend, with minimum contents at 11CB and an increase in the Bo horizons.

4.2.7. WEATHERING TREND AND PARENT MATERIAL AFFILIATION BASED ON TERNARY PLOTS.

The ternary plot SiO_2-Al_2O_3-Fe_2O_3 (Figure 11a) approximates the degree of alteration for lateritic soils; the main oxides are distributed in the top of the diagram where is the kaolinite zone (defined from the 80% of SiO_2). The samples are plotted in the right side of the triangle, according to relatively small amounts of iron (<10%) and the relative progressive enrichment in Al_2O_3. The 2C/3C horizons present the most secluded distri-

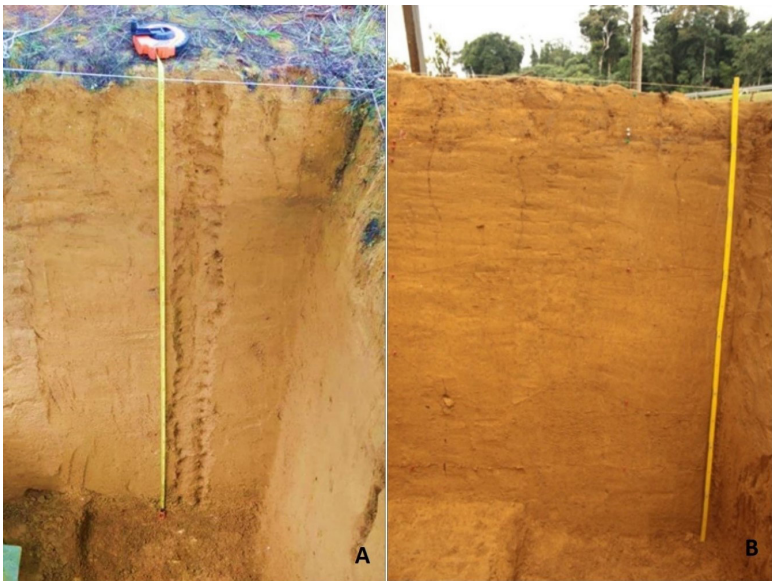

Figure 7 South (A) and West (B) profiles. It is observed that the morphological characteristics of the stratigraphic sequence are very homogeneous. Archaeological artifacts were located at the base of the profile.

http://dx.doi.org/10.18268/BSGM2022v74n3a200622

Table 2. Field description of "Mabewele I" profile.

Horizont/ Depth (cm)	Structure	Aggregate Stability	Porosity	Texture	Bioturbation	Dry color	Wet color	Boundary	Observations
Bo (0-15/18)	Subangular blocks coarse and medium	High.	Low, micropores	Silty clay.	Some fresh roots.	10YR 6/6 brownish yellow	10YR 5/6 yellowish brown	Clear and irregular.	Fe nodules, carbon and concretions of silica and gibbsite.
2C (15/18 – 21.5/26.5)	Homogeneous and compact layer of coarse white material deposited by surface flow.	Low	Low	Loamy sand	Roots, modern and ancient	Undetermined	Undetermined	Clear and irregular.	Formed by redeposited quartz sands, with an intermediate whitish layer. The thickness is varying from 0.5 to 1.5 cm and covers horizontally an extended area. It has a light inclination of 3 to 5° in a direction from NW to SE. Hard but very breakable
3C (21.5/26.5 – 24.5/31.5)	Laminate, very compact, firm and hard	Low	Low	silt	Roots	undetermined	undetermined	Clear and irregular	Very similar to the upper one, has the same inclination from NW to SE.
4Bo (24.5/31.5 – 32.5/35)	Subangular blocky.	High	Low	Silty clay	Roots	10YR 6/6 brownish yellow	10YR 5/6 yellowish brown	Diffuse	There are indurated iron concretions of dendritic shape.
5Bo (32.5/35 – 45/48)	Subangular blocks			Sandy clay	Very fine roots	10YR 6/6 brownish yellow	10YR 5/6 yellowish brown	Diffuse	Some white concretions of elongated and rounded shapes. There are single graves and carbon
6Bo (45/48 – 67.5/74.5)	Coarse and medium subangular blocks		Some pores of roots	Silty clay	Fine roots	10YR 6/6 brownish yellow	10YR 5/6 yellowish brown	Diffuse	Some silica concretions
7Bo (67.5/74.5 – 117.5/124.5)	Medium subangular blocks			Silty clay	Fresh thin roots	10YR 7/6 yellow	10YR 6/6 brownish yellow	Diffuse and irregular	Few concretions of white material
8Bo (117.5/124.5 – 135)	Medium subangular blocks	Low		Silty clay	Few fin roots.	10YR 7/6 yellow	10YR 6/6 brownish yellow	Diffuse and irregular	Soft and easy to break
9Buo (135 – 160)	Coarse and medium subangular blocks		Low and pores are very fine.	Loamy clay	Thin and strongly decomposed roots.	10YR 7/6 yellow	10YR 6/6 brownish yellow	Clear and irregular.	There are common iron nodules of medium and fine sizes and the occurrence and size rise with depth. In this zone there is a higher concentration of archaeological artefacts of different sizes (from 0.5 to 7 cm), as well some quarts fragments highly decomposed.
10Bco (160 – 165)	Medium subangular blocks	High	Low	Loamy clay	Fine roots	thin and strongly decomposed roots.	10YR 6/6 brownish yellow	Soft with a clear transition.	Enriched in iron nodules and together with iron oxides precipitation it forms "*Stone line*". Approximately 90% of the horizon is represented by Iron coarse nodules. There are some quartz intrusions of 2 cm size in average.
11CB (165 – 173)	Strongly decomposed granitic saprolite			Soft consistence			Predominantly rose pink		Preserves the original structure (medium grains,

http://dx.doi.org/10.18268/BSGM2022v74n3a200622

bution by the maximum concentration of SiO_2; the most indicative sequence of a weathering trend is defined by the mobility of SiO_2 from the 11CB horizon (saprolite) to the lower part of the triangle (where a more regular lineal cluster of the rest of the horizons reach silicon depletion and Al maxima).

The ternary plot Zr-Cr-Ti (Figure 11b) was defined by the interaction of less mobile elements in felsic rocks and its sensitivity to determine the possible parent material. The bias to the left side of the triangle is clear, where the relationship between Ti and Zr shows affinity, as well as a lower Cr concentration compared to 2C/3C and 11CB horizons.

4.2.8. RADIOCARBON DATING

Some soil samples were processed to obtain 14C AMS dating of humic acids, however, the TOC content was extremely low, and the roots of modern trees were observed throughout the profile, even in the deep parts, which made it impossible to get reliable data. A charcoal fragment from 9Buo horizon was analyzed, resulting in an age of 12572-12244 Cal BP (Table 5).

4.2.9. MICROMORPHOLOGY

Micromorphological analysis showed that, in general, the groundmass throughout the sequence is composed of coarse to fine sand, with a predominance of quartz and quartzite lithic fragments, and some micas (muscovite) in an iron-clay fine material. The coarse particles are angular and irregular and have different degrees of weathering (Figures 12a-12f). Weathered muscovite grains still retaining their laminar structure were observed (Figures 13a and 13b). Evidence of recent biological activity was also observed

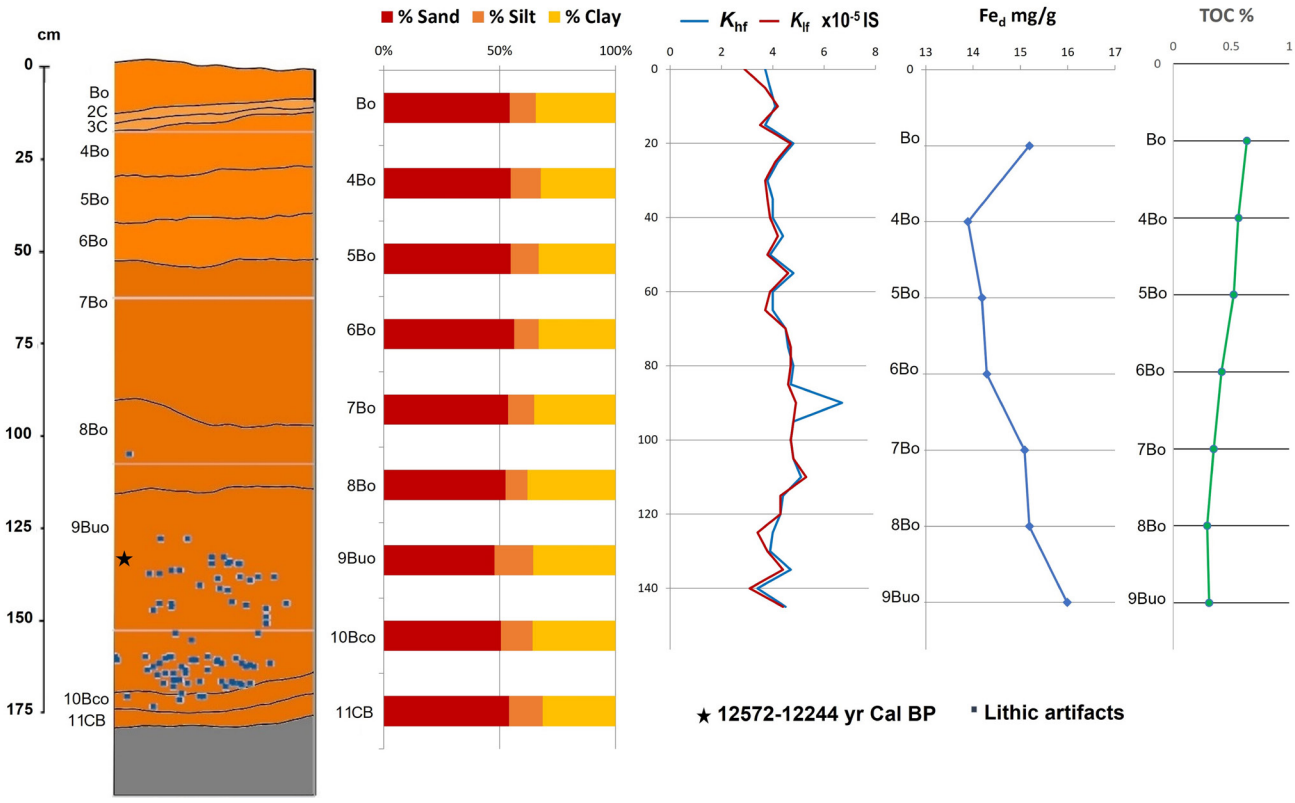

Figure 8 Scheme of the "Mabewele I" profile with the analytical results. The MSA diagnostic artifacts location in the sequence (in 9Buo) and the contents of texture, magnetic susceptibility, free iron (Fe_d) and Total Organic Carbon (TOC) are shown.

http://dx.doi.org/10.18268/BSGM2022v74n3a200622

Table 3. XRD of total samples.

Sample	Identified phases	SemiQuant RIR	Observations
Bo	Quartz: SiO_2 Kaolinite: $Al_2Si_2O_5(OH)_4$ Gibbsite: $Al(OH)_3$	87 9 4	Quartz dominance. No peaks left to identify
4Bo	Quartz: SiO_2 Kaolinite: $Al_2Si_2O_5(OH)_4$ Gibbsite: $Al(OH)_3$	90 7 3	Quartz dominance. No peaks left to identify

throughout the profile, such as root growth and fresh plant material, even in the deep horizons (Figure 12b).

The fine materials along the profile present an abundance of clay having orange-red color due to ferruginous pigment. The soil below the layers of redeposited material (2C and 3C) showed some thin clay coatings in the pores (Figures 12c and 12d), that indicate incipient illuviation. All the horizons have ferruginous nodules, but in the upper horizons the nodules are anortic (Figures 12e and 12f), *i.e.*, they appear to be reworked and fragmented complex nodules (see Stoops and Marcelino, 2018). Only in the 10Bco horizon abundant rounded concentric complex nodules formed *in situ* were observed (Figure 13e).

The 10Bco horizon is composed of saprolite fragments (metamorphized granite and granulitic gneiss) covered with iron-clay fine material (Figures 13c and 13d) in a clay matrix with a significant accumulation of complex iron nodules that present laminations (Figure 13e). This horizon also contains feldspars altered to kaolinitic clays; quartz, weathered phyllosilicates such as biotite and chlorite, as well as biogenic structures.

Finally, the basal saprolite (11CB) originates from metamorphized granite, as observed in 10Bco (Figures 13c and 13d), with a high degree of weathering and neoformation of clays and iron oxides (Figure 13f).

These rocks are composed of quartz, altered feldspars mostly replaced by kaolinites (pseudomorphs), amphiboles and micas, substituted by iron oxides and clays due to weathering *in situ* (Figures 13g and 13h).

4.2.10. PHYTOLITHS ANALYSIS

Phytoliths were recovered from seven horizons along the sequence from top to bottom (Bo to 9Buo). Eight different groups were morphologically separated: cylindrical, cylindrical scrobiculate, cylindrical crenate, cylindrical elongated, globular granular, spherical faceted, spherical with irregular folded surface and not identified (Figure 14).

9Buo and 8Bo are very similar in presence and variety of the phytoliths. All the previous morphologies are present in the two deepest layers, however only the spherical with irregular folded surface were recovered from these two layers. Its morphology is associated to *Marantacea*, *Zingiberaceae or Cannaceae* families (Runge, 1999; Piperno, 1988). The globular granulated type is predominant, and it also belongs to the same families named before (Barboni *et al.*, 2007).

7Bo, 6Bo and 5Bo had no presence of the spherical with an irregular folded type, but the other morphologies are still present. There is an important rise on globular granulated, which indi-

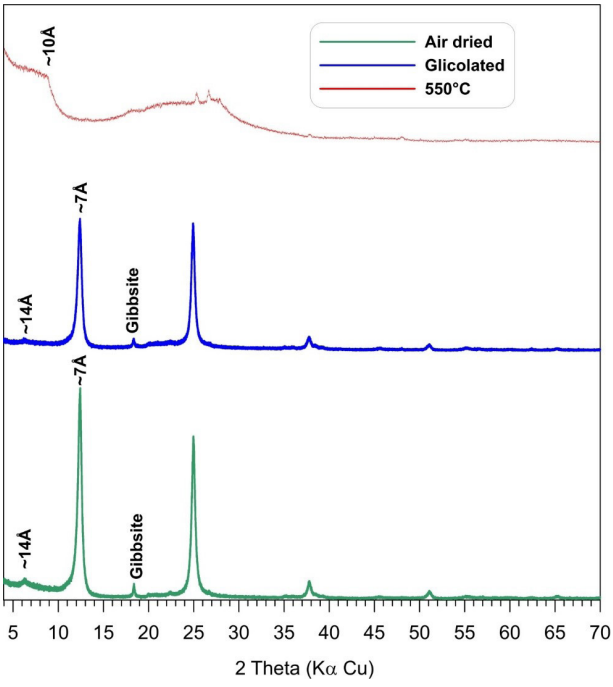

Figure 9 Diffractograms of the oriented, glycolated and heated to 550°C fractions of the 10Bco horizon, with a predominance of Kaolinite (7Å), vermiculite (10Å and 14Å) and gibbsite.

http://dx.doi.org/10.18268/BSGM2022v74n3a200622

Table 4. Identification of clays by XRD.

Sample	Peaks without treatment	Peaks with ethylene glycol	Peaks at 550°C	Identified Phases	Observations
Bo	≈7Å ≈14Å	≈7Å ≈14Å	X ≈10Å	Kaolinite Vermiculite	There are no peaks left to identify.
4Bo	≈7Å ≈14Å	≈7Å ≈14Å	X ≈10Å	Kaolinite Vermiculite	There are no peaks left to identify.
5Bo	≈7Å ≈14Å	≈7Å ≈14Å	X ≈10Å	Kaolinite Vermiculite	There are no peaks left to identify.
6Bo	≈7Å ≈14Å	≈7Å ≈14Å	X ≈10Å	Kaolinite Vermiculite	There are no peaks left to identify.
7Bo	≈7Å ≈14Å	≈7Å ≈14Å	X ≈10Å	Kaolinite Vermiculite	There are no peaks left to identify.
8Bo	≈7Å ≈14Å	≈7Å ≈14Å	X ≈10Å	Kaolinite Vermiculite	There are no peaks left to identify.
9Buo	≈7Å ≈14Å	≈7Å ≈14Å	X ≈10Å	Kaolinite Vermiculite	There are no peaks left to identify.

Table 5. Radiocarbon dating.

Horizon	Dated material	Depth (cm)	^{14}C Conventional age	^{14}C Calibrated age BP (2 σ)	Median probability	$\delta^{13}C$
9Buo	Charcoal	130	10497± 35	12572-12244	12474	-20

cates the continuity of *Marantaceae* in the middle of the sequence. Cylindrical, crenated and elongated *Poaceae* phytoliths morphologies (Bremond *et al.*, 2008) are present all along the sequence and don't have many changes in quantity except for the large cylindrical type, which gradually rises from 9Buo to the top.

4Bo and Bo have less morphological variety compared to the other horizons. Elongated, large cylindrical, hair and scrobiculated were found.

5. Discussion

5.1. INTERPRETATION OF THE PEDOLOGICAL CHARACTERISTICS OF "MABEWELE I"

The field and laboratory evaluation of the analyzed pedological materials showed that they have very similar characteristics throughout the sequence. At first glance, it appears to be a well-developed soil, with a deep B horizon, typical of tropical regions, where the formation of well-developed soils is common, with accumulation of clay minerals, quartz as well as iron and aluminum oxides and hydroxides, forming plinthic or lateritic soils (FAO, 2006; Stoops and Marcelino, 2018). Previous research indicates that in Equatorial Guinea the most common soil groups are Ferralsols, Acrisols, Nitisols and Plinthosols (De Castro y De la Calle, 1985; IUCN, 1991; Da Costa *et al.*, 2015); all of them characterized by a high degree of weathering, accumulation of clays also iron and aluminum oxides.

However, despite being in a rainforest that has remained little changed from the Miocene (Hamilton, 1976; Hamilton and Taylor, 1991; Plana, 2004), the pedogenic features of the

http://dx.doi.org/10.18268/BSGM2022v74n3a200622

Mabewele deposit do not coincide with those of the mentioned soils. Rather, the materials present a set of contrasting characteristics. On the one hand, they have a high content of clays also iron and aluminum oxides, iron nodules, kaolinites, accumulation of alumina, and on the other hand, they have a high content of sand, abundance of non-oriented fine clay material, and anorthic iron nodules, which indicate redeposition and the addition of weathered geological material to the clay soil matrix. Further evidence for the reworking is provided be the ternary diagram Zr-Cr-Ti, which shows rather close location of the majority of Bo horizons whereas the saprolite sample is rather distant from this cluster – that means a major lithological discontinuity between these two parts of the profile. Another discontinuity is shown by 2C and 3C horizons which are clearly enriched with the redeposited quartz sand material and contain a whitish interlayer.

These characteristics indicate that Bo horizons consist of reworked material, but the coarse particle morphology and size heterogeneity indicate very short transport, so the material probably comes from the higher areas (see Figures 2 and 3). Likewise, the materials show incipient pedogenetic processes after their deposition, such as the blocky structure, *in situ* weathering of some minerals, root

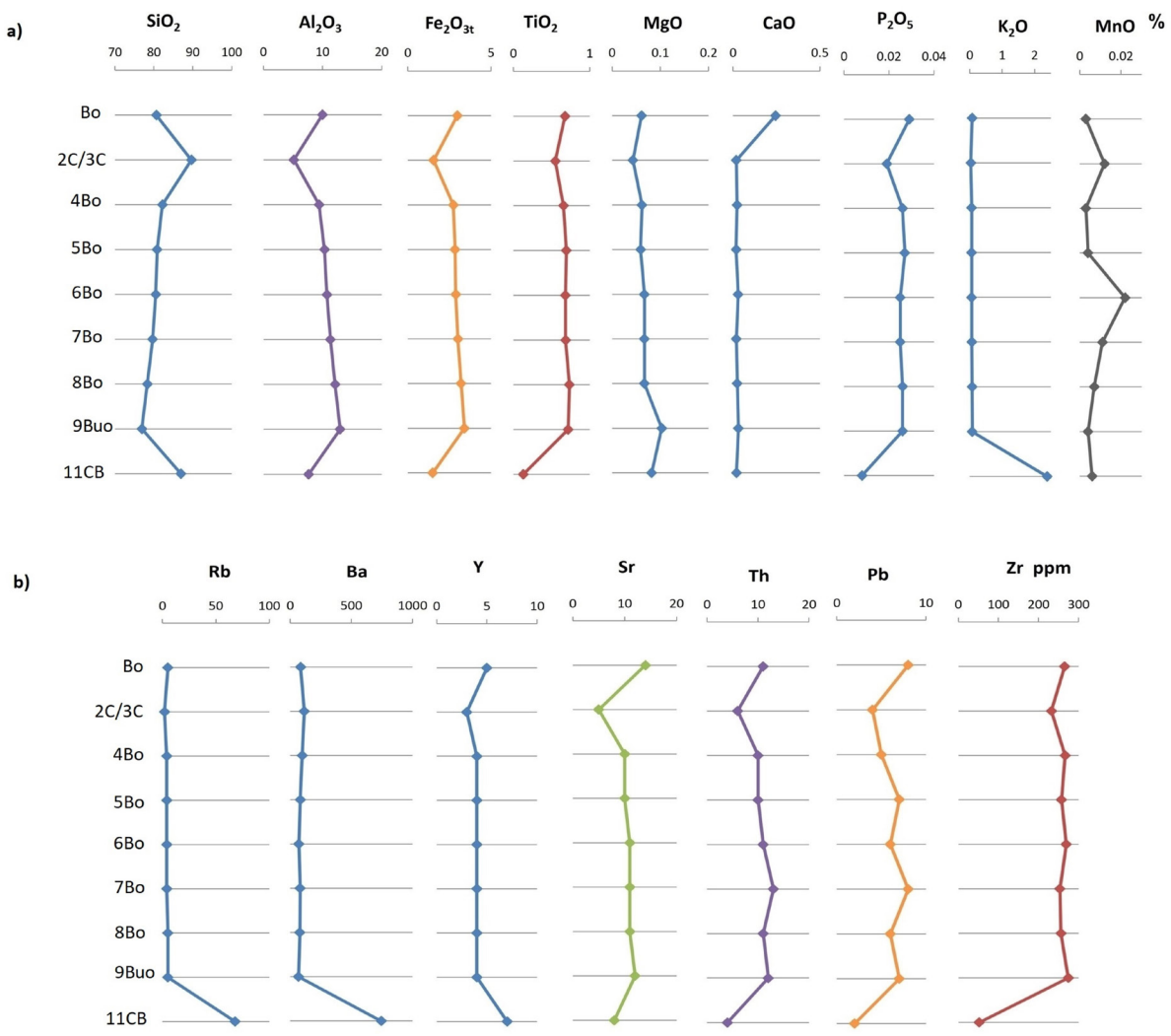

Figure 10 a) XRF analysis. Total elements (%). Small variations are observed along the profile; b) Trace elements in parts per million (ppm). A clear difference is observed between saprolite and the redeposited quartz sand layers (11CB, 3C and 2C), with the soil horizons.

http://dx.doi.org/10.18268/BSGM2022v74n3a200622

pores, oriented clays, and even formation of very incipient clay cutans in some horizons, as in 4Bo (Figures 12c and 12d). To explain the characteristics of the materials, it is possible to consider that the old soils formed in the upper areas were eroded and deposited in the lower parts, forming pedosediments. However, once deposited, they formed new surfaces and continued their pedological evolution. First this is evidenced by the geochemical data. The ternary diagram SiO_2-Al_2O_3-Fe_2O_3 demonstrates that the Bo horizons are much more weathered than the underlying saprolite. It is interesting however that the degree of weathering is highest in the lower Bo horizons (especially in the 9Buo which contains archaeological materials) and decreases in the upper horizons. This tendency culminates in the 2C and 3C horizons which are even less weathered than the saprolite. We think that it means that the balance between weathering from one side and incorporation of less altered material due to erosion/sedimentation from the other side shifted throughout deposition of the sequence in favor of the latter processes.

The predominant clays are kaolinites, with very small amounts of vermiculites. Various studies have shown that pedogenic kaolinite and gibbsite are formed by intense and prolonged weathering, being a common component in long-developing tropical soils (Stoops *et al.*, 2018); while vermiculite is more common in soils of moderate evolution, so clays show different pedogenetic periods. Kaolinites originate from the prolonged weathering of feldspars whereas vermiculites - from the transformation of micas consisting in the loss of interlayer K and lowering of the charge of unit-cell (Dixon and Weed, 1989), they could further be substituted by kaolinite. Vermiculites are common in soils with moderate development, while kaolinites are the products of the advanced alteration, therefore they are found in highly developed soils.

This mineralogical sequence was documented in a soil toposequence in Zaire: kaolinite was dominant in the lateritic soils of flat old upland surfaces whereas 2:1 clay minerals (vermiculite and smectite) appeared in the soils of steep slopes. These slopes were produced by recent (10 ka BP) incision which exposed the lower less weathered saprolite horizons and even unweathered bedrock – shists and greenstones (De Conink *et al.*, 1986). We conclude that the matrix of the set of B horizons incorporating and overlying palaeolithic findings consists predominantly of highly weathered materials with admixture of the less advanced weathering products. Such admixture could be result of incorporation of less altered materials when erosion and redeposition reached deeper saprolite horizons.

Micromorphological observation showed a high content of quartz, from the decomposition of the basal rock (quartzite and gneiss, abundance of non-oriented clays, and some oriented clays, formed by *in situ* weathering and incipient illuviation processes, in addition to concretions and iron nodules. Two types of iron nodules were observed: on the 10Bco horizon there are complex nodules, joined together by rolled iron cutans, formed *in situ* by weathering and illuviation of iron oxides towards the lower parts (Marcelino *et al.*, 2018), which formed the "stone line" on which archaeological materials were found; and in the overlying horizons, anortic nodules formed by fragments

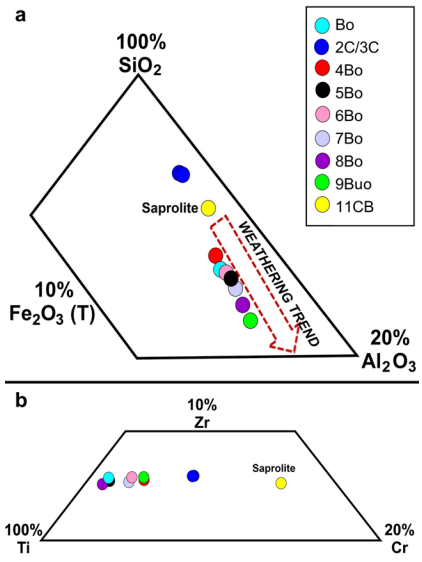

Figure 11 a) Ternary plot of SiO_2-Al_2O_3-Fe_2O_3 for general weathering trends; b) Ternary plot Zr-Cr-Ti showing affinity to parental material.

http://dx.doi.org/10.18268/BSGM2022v74n3a200622

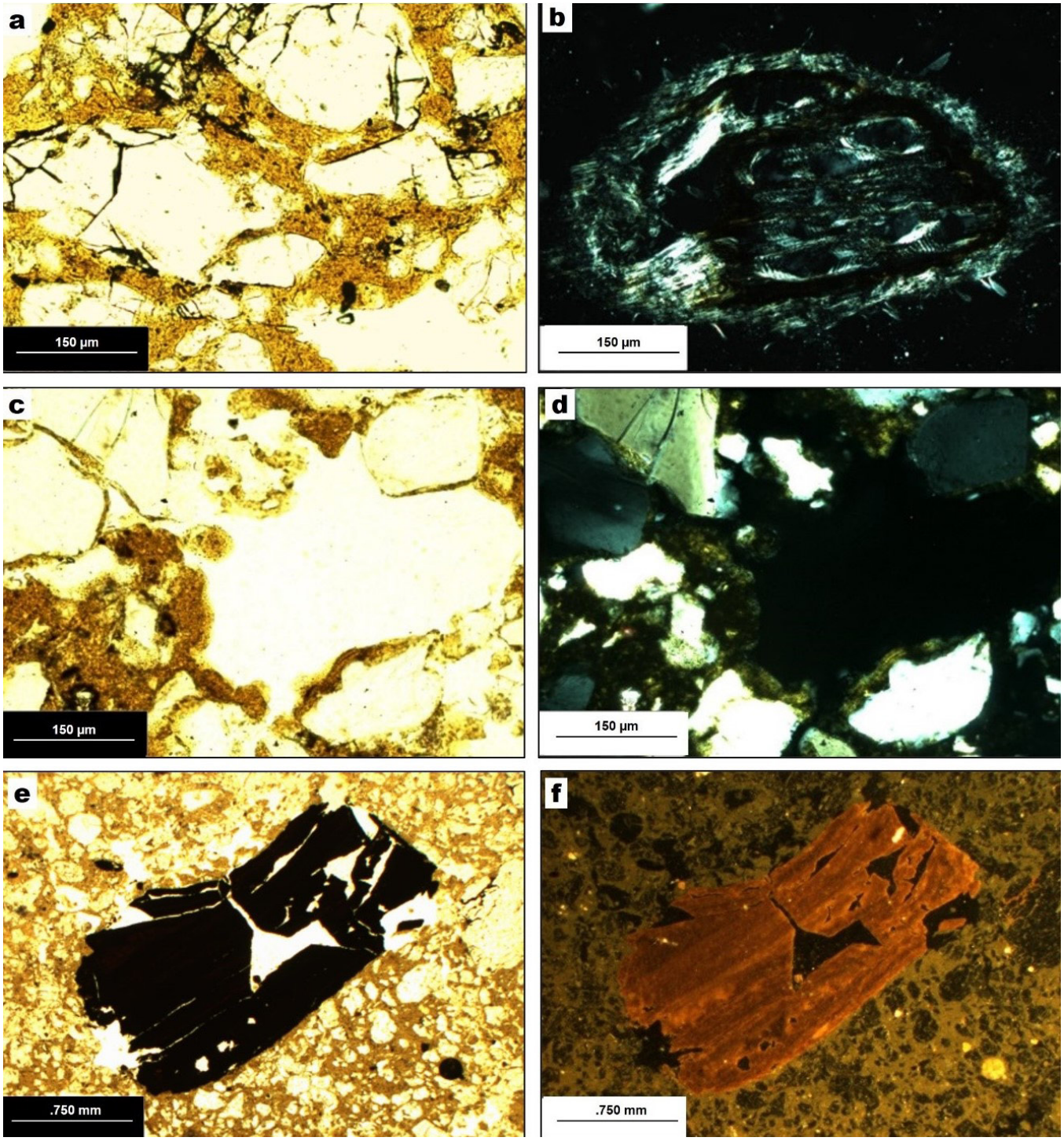

Figure 12 a) Minerals with moderate weathering and clay matrix in Bo, PPL; b) cross section of a fresh root in 8Bo, PPL and XPL; c and d) incipient clay cutan in pore, in 4Bo, PPL and XPL; e and f) iron cutans reworked in Bo, PPL and reflected light.

http://dx.doi.org/10.18268/BSGM2022v74n3a200622

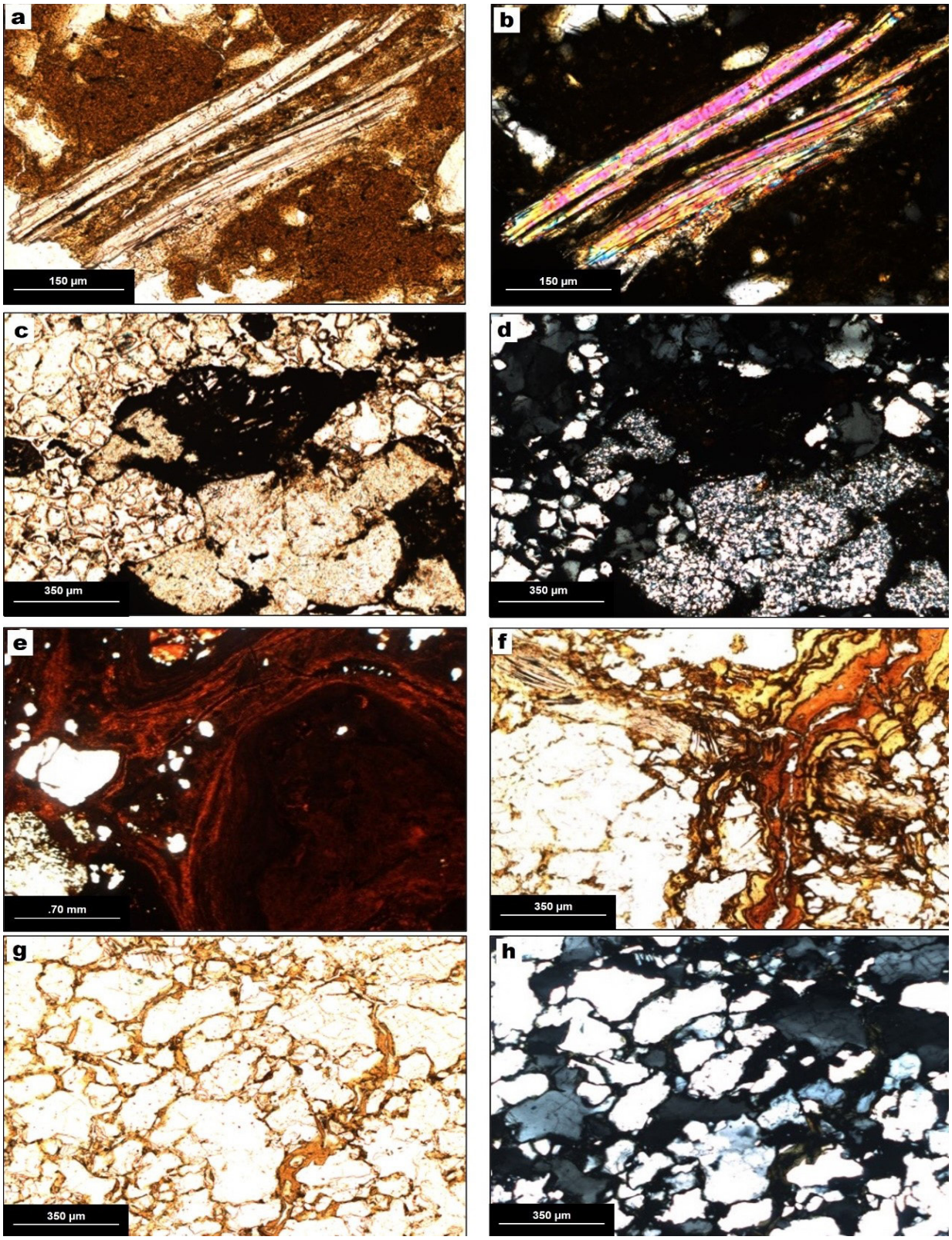

Figure 13 a) and b) Muscovite with incipient weathering in 9Buo, PPL and XPL; c and d) quartz and clay in 10Bco, PPL and XPL; e) complex iron nodules in 10Bco, PPL; f) saprolite with quartz, micas, and clay cutans in 11CB, PPL; g and h) saprolite with neoformation of clays in 11CB, PPL and XPL.

http://dx.doi.org/10.18268/BSGM2022v74n3a200622

of the complex nodules, eroded from the upper areas.

Phytoliths were mainly separated into three groups: *Poaceae*, *Marantaceae*/*Juncaceae* and *Annonaceae*. *Marantaceae* is an herbaceous plant that proliferates abundantly in disturbed areas and reduces the development of other species due to competition for space (Lima and Moura, 2006). The areas dominated by *Marantaceae* have a different plant species composition than other areas where it is not abundant (Maranho and Salimón, 2015). The fact that this family of plants is only found in the initial and middle horizons allows us to consider that their deposit conditions presented local variations in environmental humidity conditions that, in turn, promoted changes in the composition of the local vegetation cover. In summary, the analytical results showed that the profile that buries the archaeological materials of the MSA is composed of pedosediments that were formed by the erosion of soils from the higher areas, towards the lower areas, so to a large extent, the morphological characteristics of the pedosediments are inherited. Also, the characteristics observed in 10Bco and 11CB allow us to consider that the saprolitized rocks (Zauyah *et al.*, 2018) at the base of the sequence are the source of all the components observed in the pedosediments.

Likewise, the pedosediments show that, contrary to what was expected for a rainforest of great antiquity, the soils were affected by erosion-sedimentation processes in a dynamic way. To explain the origin of such processes there is a need for more specific studies on the geomorphological dynamics of the area. Given the location of Equatorial Guinea, tectonic and / or volcanic activities (Molerio, 2014) are important factors that could trigger processes of periodic erosion and re-deposition of sediments, as well as the contribution of some less degraded minerals to the oldest materials due to weathering and erosion of the rocks to be exposed by such activity. Another

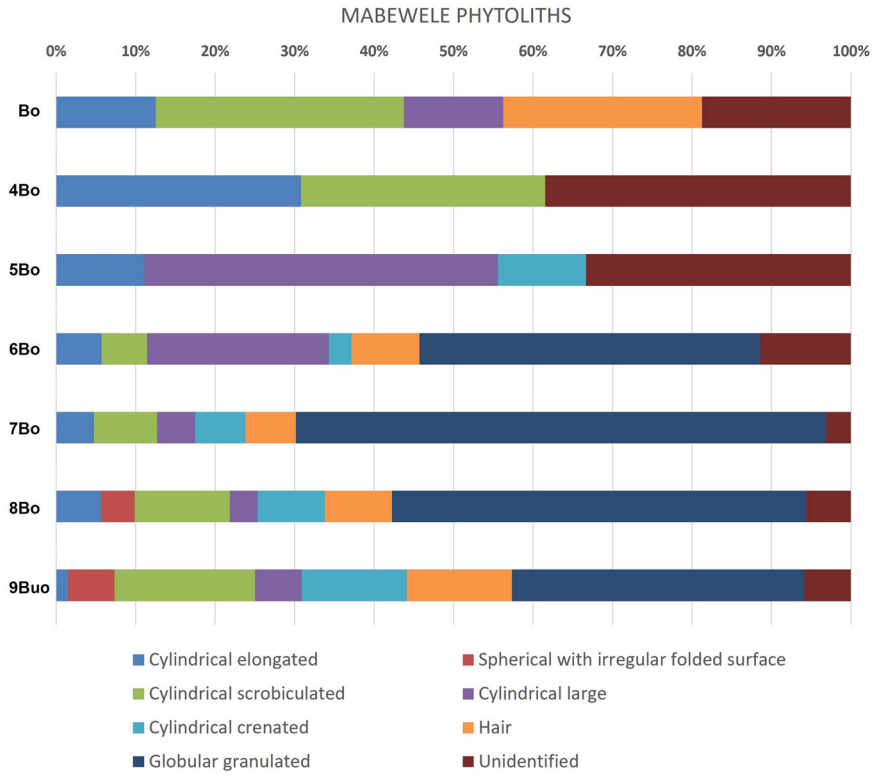

Figure 14 **Phytolith distributions (percentage) in Mabewele I profile.**

http://dx.doi.org/10.18268/BSGM2022v74n3a200622

factor to consider is the impact by marine eustatic variations related to climatic changes during the last glaciation, particularly those that occurred during the last 35 ka, which include the ending of MIS3 and MIS2 isotopic stages. Globally, it is considered that in the Last Glacial Maximum the sea level decreased approximately 120 meters with respect to the current level (Uriarte, 2004). These changes must have altered groundwater levels due to the modification of the coastlines; some regions become arid while in the equatorial zones precipitation increased, modifying the river drainage, and the erosion-sedimentation processes.

The charcoal recovered from the 9Buo horizon has an age of from 12.57-12.24 ka Cal BP; however, the charcoal was inside of the pedosediment, so it could be redeposited, in which case it would be a minimum age for the deposition of the materials. Either way, archaeological materials in 9Buo horizon are older, considering the chronological range of lithic technology (MSA). In this regard, some pedogenetic processes observed in paleosols, such as neoformation and accumulation of clays and iron oxides, formation of nodules and concretions, high weathering rates, kaolinite and gibbsite formation, are processes that develop over time prolonged (10^4 years or more) (Targulian and Krasilnikov, 2007). Pedosediments present some very incipient pedogenic processes in the upper horizons, but they are observed a little more developed towards the base of the profile (for example, complex iron nodules in 10Bco horizon), indicative of the older age of the lower horizons. Likewise, the archaeological materials identified correspond to lithic industries with an age of 250-30 ka BP (Mercader, 1995; Mercader and Marti, 1999; Mercader *et al.*, 2002; Terrazas and Rosas, 2016). So, the deposit was formed in the late Pleistocene.

5.2. THE "MABEWELE I" SITE IN THE CONTEXT OF CLIMATE CHANGE AND HUMAN OCCUPATION OF THE PLEISTOCENE IN AFRICA

As has been documented, the paleoenvironmental evolution of the tropical rainforest in Equatorial Guinea has been little studied, because it is considered that the rainforest in this area has not been affected by the climatic oscillations (Hamilton, 1976; Hamilton and Taylor, 1991; Plana, 2004). Climate changes have been studied in East Africa (Ivory and Russell, 2016), South Africa (Burrough and Thomas, 2013), Central Africa (Martí, 1999; Gasse *et al.*, 2008; Hamilton and Taylor, 1991); Gulf of Guinea (Elanga *et al.*, 1994; Weldeab *et al.*, 2007; Burrough and Thomas, 2013, Akinnigbagbe *et al.*, 2018), and Congo (Elanga, 1992; Elanga *et al.*, 1994) and Cameroon y Ghana (Maley, 1991) (Table 6).

In the same way, it is considered that the human colonization of the rainforest strip of Central Africa occurred very late, possibly at the end of the Pleistocene or, even until the Holocene. However, archaeological finds at "Mabewele I" reinforce previous research in central Africa, showing human presence in the rainforest in the Upper Pleistocene (Mercader, 1995; Mercader and Marti, 1999; Mercader *et al.*, 2002; Terrazas and Rosas, 2016).

Previous paleoenvironmental studies (summarized in Table 6) have shown that regional climate fluctuations in Africa in the Pleistocene are strongly influenced by migration from the intertropical convergence zone (ITCZ), shifting atmospheric circulation cells, and monsoon movements (West African Monsoon, Northerly East African monsoon and Southerly East African monsoon) and generally coincide with global trends: in some regions arid and open landscapes developed during the glacial and stadials periods, while during the interglacial and interstadials periods the rains increased and the forest landscape prevailed again (Weldeab *et al.*, 2007; Gasse *et al.*, 2008; Martí, 1999; Burrough and Thomas, 2013; Ivory and Russell, 2016; Akinnigbagbe *et al.*, 2018).

Studies in Equatorial Guinea focused on establishing environmental changes in the Pleistocene are scarce, but it has been established that in Central Africa - which currently shares the same tropical rainforest biome as Equatorial Guinea - climatic fluctuations should have promoted change in the landscape and vegetation, although the extent and distribution of such changes has

http://dx.doi.org/10.18268/BSGM2022v74n3a200622

not been evaluated. Palaeoenvironmental studies in Central Africa have shown climatic fluctuations that can be correlated with established marine isotopic stages –MIS– (Imbrie *et al.*, 1984), showing global climatic trends during the late Pleistocene: the Maluekian period (70-40 ka BP) is a cold and dry period that coincides with MIS4 and MIS3; the Njilian period (40-30 ka BP) is warm and humid, coinciding with MIS3; the Leopoldvillian period (30-12 ka BP) is also cold and dry, coinciding with MIS2; and finally, the Kibanguian period (12 ka BP to the present day), which coincides with MIS1 (Martinson *et al.*, 1987; Martí, 1999). Although sediments from Bosumtwi (Ghana) and Barombi Mbo (Cameroon) lakes and the Gulf of Guinea show cooling and decrease in precipitation during the LGM (22 ka BP) and Younger Dryas –YD- (12.7 - 11.7 ka BP) periods (Gasse *et al.*, 2008), the "Mabewele I" pedosedimentary sequence shows no changes in its characteristics that can be correlated with these climatic fluctuations. In this case, the materials show only minor variations along the sequence, indicating that the environmental conditions did not have important changes. These data correlate with the studies of marsh sediments in the Bateke Plateau and coastal areas of the Congo, where the presence of hydromorphic forests has been observed for 24 ka, showing a humid phase; between 24-13 ka BP there is expansion of swamp communities due to a slightly drier climate, but not arid as has been observed in other regions, followed by another wet period after 13 ka BP (Elanga, 1992; Elanga *et al.*, 1994). Likewise, the pollinic sequence of Lake Marombi Mbo showed that the tropical rainforest persists (although with small variations) since 24 ka BP, for which it is considered a refuge area for the tropical rainforest (Maley, 1991).

Based on typological comparisons whit others sites in Equatorial Guinea (Mercader and Martí 1999, 2002), the archaeological artifacts recovered at the base of the profile have a minimum age of 30 ka BP and their characteristics (sharp edges, fragments that can rearticulate) indicate little or no erosion and were located on a paleosol *in situ* (horizon 10Bco), so the overlying horizons (9Buo and 8Bo) were formed between 30 -12.5 ka BP, since charcoal obtained from the 9Buo horizon was dated between 12.57-12.24 ka Cal BP. Therefore, the upper horizons would have been formed in the Holocene. As already mentioned, the similarity in the characteristics of the Pleistocene and Holocene pedosediments indicate similar environments, which is consistent with various studies in marine and lake sediments, which have shown that in the equatorial zone (Central and East Africa) the climate during the Last Glacial Maximum (LGM) was drier than today, with a reduction in forested areas in the southeast of the continent (Tanganyika Lake), while in the west (Guinea Gulf, Bateke Plateau, Congo) higher humidity prevailed, maintaining a tropical ecosystem (Elanga *et al.*, 1994; Gasse *et al.*, 2008; Ivory and Rusell, 2016). We suppose that the latter tendency also prevailed in the studied area.

However, as discussed in the previous section, the soils of the "Mabewele I" site do not show the characteristics of the soils developed for a long time under a stable tropical environment, but rather evidence periods of pedogenesis-erosion/sedimentation-pedogenesis. Previous studies (Hamilton, 1976; Maley, 1991; Elanga, 1992; Elanga *et al.*, 1994) indicate that the tropical ecosystem prevailed in the Equatorial Guinea area, so that although there was a decrease in precipitation, the environmental conditions would not vary too much, then, they would not be sufficient to promote the dynamics of disturbance and soil erosion observed in "Mabewele I".

Therefore, it is necessary to also consider that the affectations to the pedological cover due to the establishment of the human groups during the Middle Stone Age may constitute a relevant factor for the changes in the geomorphological dynamics, since by taking advantage of the natural resources of their environment and carrying out activities such as hunting and gathering, construction of bonfires and shelters, among other, impacted the soils and vegetation cover, favoring soil erosion and the formation of pedosedimentary sequences in the lower terraces (for an example of hunter-gatherers impact in different kinds of tropical forests see Head, 1996).

Table 6. Climate trends in Africa, based on previous studies.

MIS[1]	Global Climate trends	Southern Nigeria (Akinnigbagbe *et al* 2018)	Lake Bosumtwi, Ghana and Lake Barombi Mbo, Cameroon (Maley, 1991)	Congo (Elanga, 1992; Elanga et al, 1994)	Gulf of Guinea and Congo Basin (Gasse *et al*, 2008)	Gulf of Guinea (Burrough & Thomas, 2013)	Central Africa (Hamilton & Taylor, 1991)	West Africa (Hamilton, 1976)	Central Africa (Martí, 1999)	Lake Tanganyika (Ivory & Russell, 2016)	Albertine Rift (Hamilton & Taylor, 2018)
1 11.7 ka BP - present	Warm and wet	Wet weak trade winds ITCZ[2] to the north	9 ka BP the montane vegetation is replaced by the tropical forest, the warm and humid period begins		EH[3] wetter and warm conditions	14.8 - 5.5 ka African wet period. West African monsoon	Wetter and warm conditions		Kibanguiense B Period. 0-4 ka BP Current climate. Kibanguiense A Period. 4-12 ka BP Warm and wet		
2 11.7 - 27 ka BP	Cold and dry	less precipitation and strong trade winds, ITCZ to the south	24 ka BP Lake Barombi Mbo. Warm and humid period, the tropical forest persists since then. 28 – 9 ka BP Lake Bosumtwi cold and wet period, the montane vegetation displaces the tropical forest.	13 ka AP begins new wet period 24-13 ka AP slightly drier period 24 ka AP wet period	YD[4] 12.7 ka BP cold and dry, ITCZ to the south 15-12.9 ka BP wet 17–16 ka BP wet and cold LGM[5] 22 ka BP cold and dry, ITCZ to the south		21 – 12 ka BP cold and dry, with centers of forest survival in Cameroon-Equatorial Guinea-Gabon, eastern Zaire, Sierra Leone-Liberia, East Ivory coast-West Ghana and East African coast	20 ka BP dry and cold, reduction of the lowland forest to some refuge centers, among them Cameroon-Equatorial Guinea-Gabon and eastern Zaire	Leopoldovillense Period 12-30-ka BP Cold and dry	LGM drier than today. Forest reduction in southeast Africa, but wet condition in southwest Africa.	Depressed temperatures then continued until the transition to a postglacial climate dating to about 14 – 11.5 ka BP
3 27 - 59 ka BP	Warm and wet	Wet weak trade winds ITCZ to the north							Njiliense Period 40-30 ka BP Warm and humid		43 -40 ka BP, cold and drier climate
4 59 - 74 ka BP	Cold and dry	less precipitation and strong trade winds, ITCZ to the south							Maluekiense Period 70-40 ka BP Cold and dry, with loss of vegetation.		

[1]Marine Isotopic Stage; [2]ITCZ intertropical convergence zone; [3]EH Early Holocene; [4]YD Younger Dryas; [5]Late Glacial Maximum.

http://dx.doi.org/10.18268/BSGM2022v74n3a200622

http://dx.doi.org/10.18268/BSGM2022v74n3a200622

Traditionally the palaeolithic societies are thought to produce very limited and local impact on soils and landscapes, the start of major transformation is usually associated with the neolithic revolution. However recent detailed paleoecological studies in the Northern Europe pointed to major transformation of vegetation cover: decrease of forests and extension of open grassland ecosystems due to the land use practices of the Middle Palaeolithic inhabitants as early as the previous interglacial (MIS5e) (Roebroeks *et al.*, 2021). In Tropical Africa the model of Late Pleistocene ecosystem change due to the long-term large-scale activities of the Upper Palaeolithic societies was developed by Thompson *et al.* (2021) basing on detailed lacustrine archives from Lake Malawi. We suppose that the interaction of humans with their environment during the period of the initial spread of *Homo sapiens* in the tropical zone of the African continent could produce major changes of the soils and landscapes although the subsistence of these societies was still based on hunting and gathering. Still, much more research is needed to justify this hypothesis on the regional and continental scales.

6. Conclusions

Opposite to expectations because it is a tropical rainforest, the materials that bury the archaeological artifacts of the Middle Stone Age are not highly developed soils, but rather constitute a pedosedimentary sequence that indicates great environmental dynamism. The pedosediments are formed by old soils that were eroded from the upper parts and redeposited in lower areas. This is evidenced by the high content of sands (in all cases of more than 50%) of variable grain size and morphology, which indicates short transport, mixed with a clay matrix also in quantity important (more than 30%), showing weathering and neoformation of secondary minerals, mainly before redeposition, but also after it.

The pedosediments show similar characteristics throughout the entire sequence, among which the absence of organic horizons –*in situ* or mixed with other materials– stands out. This is indicative of periods of environmental instability that promoted erosion processes, with loss of surface horizons and redeposition of pre-existing soils in the lower areas, although this instability is not associated with changes in regional environmental conditions, which do not seem to have varied greatly over time, since the high degree of weathering evaluated in the fine fraction is related to a warm and humid climate, like that prevailing today.

The characteristics of the "Mabewele I" profile suggest that human beings from the MSA may have been able to modify their environment, creating open spaces between the forest and favoring the growth of plants useful for subsistence, which, together with the use of fire and other territory management practices were able to create anthropized areas of vegetation, although everything indicates that these practices did not negatively disturb the humid forest ecosystems at the end of the Pleistocene, which have been maintained to this day.

Contributions of authors

1. Conceptualization: TCyC, ATM; 2. Analysis or data acquisition: TCyC, ATM, SS, LP, TPP, IRG, HCB; 3. Methodologic/technical development: TCyC, ATM; 4. Writing of the original manuscript: TCyC; 5. Writing of the corrected and edited manuscript: TCyC; 6. Graphic design: TCyC, ATM, HCB; 7. Fieldwork: ATM, BMI, JRR, LP; 8. Interpretation: TCyC, SS, ATM; 9. Financing: ATM.

Financing

UNAM, Project PAPIIT IN400916/UNAM; Postdoctoral Scholarship Program, UNAM.

Acknowledgments

We acknowledge the support of the UNAM Postdoctoral Scholarship Program, Institute of Anthropological Research, Institute of Geology,

Institute of Geophysics and Institute of Physics of UNAM; Project PAPIIT IN400916/UNAM, State Research Program Nº 122011800459-3 of the M.V. Lomonosov Moscow State University; Laboratorio Nacional de Geoquímica y Mineralogía (LANGEM) and Laboratorio Nacional de Espectrometría de Masas con Aceleradores (LEMA), UNAM, as well as to Ana María Soler Arechalde, Corina Solís Rosales and Jaime Díaz Ortega for the analytical assistance. We also thank the Council for Scientific and Technological Research of Equatorial Guinea (CICTE, for its acronym in Spanish), National University of Equatorial Guinea, National Institute for Forest Development and Protected Areas (INDEFOR, for its acronym in Spanish), Filiberto Ntutumu Nguema Nchama, Fidel Mba Eyono, Anacleto Oló Mbi, the authorities of the Niefang District, Mabewele and the entire community for their support during the fieldwork.

Conflicts of interest

The authors declare that they have no known competing financial interests or personal relationships that could have appeared to influence the work reported in this paper.

References

Adkins, J., deMenocal, P., Eshel, G., 2006, The "African humid period" and the record of marine upwelling from excess ^{230}Th in ODP Hole 658C: Paleoceanography and Paleoclimatology, 21(4), PA4203. https://doi.org/10.1029/2005PA001200

Akinnigbagbe, A. E., Han, X., Fan, W., Tang, Y., Adeleye, A. O., Jimoh, R., Lou, Z., 2018, Variations in terrigenous input into the eastern Equatorial Atlantic over 120ka: Implications on Atlantic ITCZ migration: Journal of African Earth Sciences, 147, 220-227. https://doi.org/10.1016/j.jafrearsci.2018.06.010

Alvar, J., Mas-Coma, S., Carrasco, M.,1996, Modern history and physical geography of Equatorial Guinea: Research and Reviews in Parasitology, 56 (2-3), 77-83.

Aydin, A., Duzgoren-Aydin, N. S., 2002, Indices for scaling and predicting weathering-induced changes in rock properties: Environmental and Engineering Geoscience, 8(2), 121-135. https://doi.org/10.2113/gseegeosci.8.2.121

Bailey, R.C., Peacock, N. R., 1988, Efe Pygmies of northeast Zaire: Subsistence strategies in the Ituri Forest, in de Garine, I., Harrison, G. A., (eds.), Coping with uncertainty in food supply: Oxford, Oxford University Press, 88–117.

Barboni, D., Bremond, L., Bonnefille, R., 2007, Comparative study of modern phytolith assemblages from inter-tropical Africa: Palaeogeography, Palaeoclimatology, Palaeoecology, 246 454–470. https://doi.org/10.1016/j.palaeo.2006.10.012

Bremond, L., Alexandre, A., Wooller, M., Hély, C., Williamson, D., Schäffer,P.,Majule, A., Guiot,J., 2008, Phytolith indices as proxies of grass subfamilies on East African tropical mountains: Global and Planetary Change, 61 (3-4), 209 - 224. https://doi.org/10.1016/j.gloplacha.2007.08.016

Buol, S. W., Hole, F. D., McCracken, R. J., 1981, Génesis y clasificación de suelos: México, Trillas, 417p.

Burrough, S. I., Thomas, D. S. G., 2103, Central southern Africa at the time of the African Humid Period: a new analysis of Holocene palaeoenvironmental and palaeoclimate data: Quaternary Science Reviews, 80, 29-46. https://doi.org/10.1016/j.quascirev.2013.08.001

COHMAP Members, 1988, Climatic changes of the last 18,000 years: Observations and model simulations: Science 241, 1043-1052. https://doi.org/10.1126/science.241.4869.104

Da Costa, P. Y. D., Nguetnkam, J. P., Mvoubou, C. M., Togbé, K. A., Ettien, J. B., Yao-Kouame,

A., 2015, Old landscapes, pre-weathered materials, and pedogenesis in tropical Africa: How can the time factor of soil formation be assessed in these regions? Quaternary International, 376, 47-74. https://doi.org/10.1016/j.quaint.2014.04.062

De Castro Antolín, M. L., De la Calle Muñoz, M. L., 1985, Geografía de Guinea Ecuatorial. Programa de colaboración Educativa con Guinea Ecuatorial: España, Secretaría General Técnica, Ministerio de Educación y Ciencia, 73p.

Dearing, J.A., Hay, K.L., Baban, S.M.J., Huddleston, A.S., Wellington, E.M.H., Loveland, P.J., 1996, Magnetic susceptibility of soil: An evalation of conflicting theories usung a national data set: Geophysical Journal International, 127, 728-738. https://doi.org/10.1111/j.1365-246X.1996.tb04051.x

Deb, B.C., 1950, The estimations of free iron oxide in soils and clays and their removal: Journal of Soil Science, 1, 212-220. https://doi.org/10.1111/j.1365-2389.1950.tb00733.x

deMenocal, P. B., Ortiz, J., Guilederson, T., Adkins, J., Sarthein, M., Baker, L., Yarusisky, M.,2000, Abrupt on set and termination of the African Humid Period: Rapid climate responses to gradual insolation forcing: Quaternary Science Reviews, 19, 347-361. https://doi.org/10.1016/S0277-3791(99)00081-5

Díaz del Olmo, F., Cámara Artigas, R., Micha Ondo, A., Domínguez Llosa, R., 2016, Modelo de conectividad norte-sur en bosque húmedo congoleño: la propuesta de Reserva de Biósfera de la Región Continental de Guinea Ecuatorial, en Gómez, J., Arias, J., Olmedo, J. A., Serrano, J. L. (eds.), Avances en biogeografía. Áreas de distribución: Entre puentes y barreras: España: Universidad de Granada, 65-73.

Elenga, H., 1992, Végétation et climat du Congo depuis 24,000 ans B.P. Analyse palynologique de séquences sédimentaires du Pays Bateke et du littoral: France, Univ. Aix-Marseille III, PhD Dissertation, 237p.

Elanga, H., Schwartz, D., Vicens, A., 1994, Pollen evidencie of late Quaternary vegetation and onferred climate changes in Congo: Palaeogeography, Palaeoclimatology, Palaeoecology, 109, 345-356. https://doi.org/10.1016/0031-0182(94)90184-8

FAO, 2006, Guidelines for soil description. 4th edition: Rome, Food and Agriculture Organization of the United Nations, 109p.

Gasse, F., Chalié, F., Vincens, A., Williams, M., Williamson, D., 2008, Climatic patterns in equatorial and southern Africa from 30,000 to 10,000 years ago reconstructed from terrestrial and near-shore proxy data: Quaternary Science Reviews, 27, 2316-2340. https://doi.org/10.1016/j.quascirev.2008.08.027

Hamilton, A. C., 1976, The significance of patterns of distribution shown by forest plants and animals in tropical Africa for the reconstruction of Upper Pleistocene palaeoenviroments: a review: Palaeoecology of Africa, 9, 63-97.

Hamilton, A. C., Taylor, D., 1991, Histroy of climate and forests in Tropical Africa during the last 8 million years: Climatic Change, 19, 65-78. https://doi.org/10.1007/BF00142215

Hart, T. B., Hart, J. A., 1986, The ecological basis of hunter-gatherer subsistence in African rainforests: the Mbuti of Eastern Zaire: Human Ecology, 14 (1), 29-55. https://doi.org/10.1007/BF00889209

Head, L., 1996, Rethinking the prehistory of hunter-gatherers, fire and vegetation change in northern Australia: The Holocene, 6(4), 481-487. https://doi.org/10.1177/095968369600600412

Headland, T. N., 1987, The wild yam question: How well could independent hunter-gatherers live in a tropical rainforest ecosystem? Human Ecology, 15 (4), 463-491. https://doi.org/10.1007/BF00888000

Hill, I. G., Worden, R. H., Meighan, I. G., 2000, Yttrium: the immobility-mobility transition

http://dx.doi.org/10.18268/BSGM2022v74n3a200622

during basaltic weathering: Geology, 28, 923-926. https://doi.org/10.1130/0091-7613(2000) 28<923:YTITDB>2.0.CO ;2

Hublin, J. J., Ben-Ncer. A., Bailey, S. E., Freidline, S. E., Neubauer, S., Skinner, M., Bergmann, I., Le Cabec, A., Benazzi, S., Harvati, K, Gunz, P., 2017, New fossils from Jebel Irhoud, Morocco and the pan-African origin of Homo sapiens: Nature, 546, 289-292. https://doi.org/10.1038/nature22336

Imbrie, J., Hays, J. D., Martinson, D. G., McIntyre, A., Mix, A. C., Morley, J. J., Pisias, N. G., Prell, W. L., Shackleton, N. J., 1984, The orbital theory of Pleistocene climate: support from a revised chronology of the marine $\delta^{18}O$ record, in Berger, A. L., Imbrie, J., Hays, J. D., Kukla, G., Saltzman, B., (eds.), Milankovitch and climate: Dordrecht, Reidel Publisher, 269-305.

IUCN, 1991, Conservación de los ecosistemas forestales de Guinea Ecuatorial, basado en el trabajo de John E. Fa: Suiza, Unión Internacional para la Conservación de la Naturaleza (UICN), 237p.

Ivory, S., Russell, J., 2016, Climate, herbivory, and fire controls on tropical African forest for the last 60 ka: Quaternary Science Reviews, 148, 101-114. https://doi.org/10.1016/j.quascirev.2016.07.015

Jackson, M.L., 1958, Soil chemical analysis: Englewood Cliffs, Prentice-Hall, 498p.

Jasso-Castañeda, C., Gama-Castro, J. E., Solleiro-Rebolledo, E., Díaz-Ortega, J., 2012, Morfogénesis, procesos y evolución del horizonte Bw cámbico en tefra-paleosuelos del volcán Nevado de Toluca: Boletín de la Sociedad Geológica Mexicana, 64(1), 37-47.https://doi.org/10.18268/BSGM2012v64n1a3

Lézine, A-M., Holl, A.F-C., Lebamba, J., Vincens, A., Assi-Khaudjis, C., Février, L., Sultan, É., 2013, Temporal relationship between holocene human occupation and vegetation change along the northwestern margin of the central african rainforest: Comptes Rendus Geoscience, 345,327–335. https://doi.org/10.1016/j.crte.2013.03.001

Lima, R.A., Moura, L.C., 2008, Gap disturbance regime and composition in the Atlantic Montane Rain Forest: the influence of topography: Plant Ecology, 197(2), 239-253. https://doi.org/10.1007/s11258-007-9374-x

Madella, M., Alexandre, A., Ball, T., 2005, International Code for Phytolith Nomenclature 1.0: Annals of Botany, 96, 253–260. https://doi.org/10.1093/aob/mci172

Maley, J., 1991, The African Rain-Forest Vegetation and Paleoenvironments during Late Quaternary: Climatic Change, 19, 79-98. https://doi.org/10.1007/BF00142216

Marcelino, V., Schaefer, C., Stoops, G., 2018, Oxic and Related Materials, in Stoops, G., Marcelino, V., Mees, F., (eds.), Interpretation of micromorphological features of soils and regoliths, 2d. Ed.: Oxford, Elsevier, 663-689.

Martí, R., 1999, La secuencia arqueológica en el cinturón forestal centroafricano: Espacio Tiempo y Forma. Serie I, Prehistoria y Arqueología, 12, 41-66. https://doi.org/10.5944/etfi.12.1999.4678

Martínez-Torres, L. M., Riaza, A., 1996, Explicación del mapa geológico de Guinea Ecuatorial Continental: Bilbao, Asociación Africanista Manuel Iradier.

Martinson, D.G., Pisias, N.G., Hays, J.D., Imbrie, J., Moore, T.C., Shackleton, N.J., 1987, Age dating and the orbital theory of the ice ages: development of a high resolution 0 to 300,000-year chronostratigraphy: Quaternary Research, 27, 1-29. https://doi.org/10.1016/0033-5894(87)90046-9

Mercader, J., 1995, La colonización del bosque lluvioso tropical centro-Africano: Complutum, 6, 105-122.

Mercader, J., 2002, Forest people: The role of African rainforests in human evolution and dispersal: Evolutionary Anthropology, 11, 117-124. https://doi.org/10.1002/evan.10022

Mercader, J., Marti, R., 1999, Middle stone age sites in the tropical forests of Equatorial Guinea: Nyame Akuma, 51, 14-24.

Mercader, J., Martí, R., Martínez, J. L., Brooks, A., 2002, The nature of 'stone-lines' in the African Quaternary record: archaeological resolution at the rainforest site of Mosumu, Equatorial Guinea: Quaternary International, 89, 71-96. https://doi.org/10.1016/S1040-6182(01)00082-9

Mehra, O. P., Jackson, M. L., 1960, Iron oxide removal from soils and clays by a dithonite-citrete system buffered with sodium bicarbonate: Clays and Clays minerals, 7, 317-327. https://doi.org/10.1016/B978-0-08-009235-5.50026-7

Molerio León, L. F., 2014, El vulcanismo en guinea ecuatorial y los peligros naturales asociados. (Vulcanism in equatorial guinea and associated natural hazards): Cub@: Medio Ambiente y Desarrollo, 14(26), 1-8.

Moore, D., Reynolds, Jr. R.C., 1997, X-Ray Diffraction and the identification and analysis of clay minerals, 2nd ed: Oxford, Oxford University Press, 400p.

Mounteney, I., Burton, A. K., Farrant, A. R., Watts, M. J., Kemp, S. J., Cook, J. M., 2018, Heavy mineral analysis by ICP-AES a tool to aid sediment provenancing: Journal of Geochemical Exploration, 184, 1-10. https:/doi: 10.1016/j.gexplo.2017.10.007

Murienne, J., Benavides, L. R., Prendini, L., Hormiga, G., Giribet, G., 2012, Forest refugia in Western and Central Africa as 'museums' of Mesozoic biodiversity: Biology Letters, 9, 1-7. https://doi.org/10.1098/rsbl.2012.0932

Ngomanda, A., Chepstow-Lusty, A., Makaya, M., Favier, C., Schevin, P., Maley, J., Fontugne, M., Oslisly, R., Jolly, D., 2009, Western equatorial African forest-savanna mosaics: a legacy of late Holocene climatic change? Climate of the Past, 5, 647-659. https://doi.org/10.5194/cp-5-647-2009

Nesbitt, H.W., Young, G.M., 1982, Early Proterozoic climates and plate motions inferred from major elementary chemistry of lutites: Nature, 299, 715-717. https://doi.org/10.1038/299715a0

Piperno, D., 1988, Phytolith analysis: an archaeological and geological perspective: San Diego, Academic Press, 280p.

Plana, V., 2004, Mechanisms and tempo of evolution in the African Guineo-Congolian rainforest: Philosophical Transactions of the Royal Society B. Biological Sciences, 359, 1585-1594. https://doi.org/10.1098/rstb.2004.1535

Rietveld, H. A.,1969, Profile refinement method for nuclear and magnetic structures: Journal Applied Crystallography, 2(2), 65–71. https://doi.org/10.1107/S0021889869006558

Roebroeks, W., MacDonald, K., Scherjon, F., Bakels, C.C., Kindler, L., NIKULINA, A., Pop, E.A.L. Gaudzinski-Windheuser, S., 2021, Landscape modification by Last Interglacial Neanderthals: Science Advances, 7 (51), eabj5567. https://doi.org/10.1126/sciadv.abj5567

Runge, F., 1999, The opal phytolith inventory of soils in central Africa —quantities, shapes, classification, and spectra: Review of Palaeobotany and Palynology, 107, 23–53. https://doi.org/10.1016/S0034-6667(99)00018-4

Sahnnouni, M., Parés, J. M., Duval, M., Cáceres, I., Harichane, Z., Van der Made, J., Pérez-González, A., Abdessadok, S., Kandi, N., Medig, M., Boulaghraif, K., Semaw, S., 2018, 1.9 million and 2.4 million year old artifacts and stone tool-cutmarked bones from Ain Boucherit, Algeria: Science, 362(6420), 1297-1301. https://doi.org/10.1126/science.aau0008

Sarnthein, M., 1978, Sand deserts during glacial maximum and climatic optium: Nature, 272, 43-46. https://doi.org/10.1038/272043a0

Sobrinho - Maranho, A., Salimón, C.I., 2015, Maranthaceae overabundance decreases richness and abundance of regenerating

http://dx.doi.org/10.18268/BSGM2022v74n3a200622

woody plants in natural gaps: Neotropical Biology and Conservation, 10(2),53-62. https://doi.org/10.4013/nbc.2015.102.01

Steele, T.E., 2013, Vertebrate records: Late Pleistocene of Africa, in Elias, S.A., Mock, C.J., (eds.), Encyclopedia of Quaternary Science (Second Edition): Oxford, Elsevier, 664-672. https://doi.org/10.1016/B978-0-444-53643-3.00247-8

Stoops, G., Marcelino, V., 2018, Lateritic and bauxitic materials, in Stoops, G., Marcelino, V., Mees, F., (eds.), Interpretation of micromorphological features of soils and regoliths, Vol. 2: Oxford, Elsevier, 691-720. https://doi.org/10.1016/B978-0-444-63522-8.00024-3

Targulian, V. O., Krasilinikov. P. V., 2007. Soil system and pedogenic processes: Self-organization, time scales, and environmental significance: Catena, 71, 373-381. https://doi.org/10.1016/j.catena.2007.03.007

Taylor, N., 2016, Across rainforests and woodlands: A systematic reappraisal of the lupemban middle stone age in Central Africa, in Jones, S.C., Stewart, B.A., (eds.), Africa from MIS 6-2: Netherlands, Springer, 273-299. https://doi.org/10.1007/978-94-017-7520-5_15

Terrazas, A., Rosas, A., 2016, A new approach to the Middle Stone Age from continental Equatorial Guinea: A preliminary fieldwork report: Nyame Akuma, 85, 129-139.

Thompson, J. C., Wright, D. K., Ivory, S. J., Choi, J.-H., Nightingale, S., Mackay, A., Schilt, F., Otárola-Castillo, E., Mercader, J., Forman, S. L., Pietsch, T., Cohen, A. S., Arrowsmith, J. R., Welling, M., Davis, J., Schiery, B., Kaliba, P., Malijani, O., Blome, M. W., O'Driscoll, C. A., Mentzer, S. M., Miller, C., Heo, S., Choi, J., Tembo, J., Mapemba, F., Simengwa, D., Gomani-Chindebvu, E., 2021, Early human impacts and ecosystem reorganization in southern-central Africa: Science Advance, 7(19), eabf9776. https://doi.org/10.1126/sciadv.abf9776

Van Zinderen Bakker, E.M., 1966, Palaeoecology of Africa & of the surrounding islands & Antarctica, Vol. 5: Cape Town, A.A. Balkema.

Velayos, M., Aedo, C., Cabezas, M., de la Estrella, M., Barberá, P., Fero, M., 2014, Flora de Guinea Ecuatorial. Claves de plantas vasculares de Annobón, Bioko y Río Muni: Madrid, Consejo Superior de Investigaciones Científicas, 491p.

Weldeab, S., Lea, D. W., Schneider, R. R., Andersen, N., 2007, 155,000 years of West African Monsoon and Ocean Thermal Evolution: Science, 316(5829), 1303-1307. https://doi.org/10.1126/science.1140461

Zauyah, S., Schaefer, C., Simas, F., 2018, Saprolites, in Stoops, G., Marcelino, V. and Mees, F., (eds.), Interpretation of micromorphological features of soils and regoliths, Vol 2nd: Oxford, Elsevier, 37-57. https://doi.org/10.1016/B978-0-444-53156-8.00004-0